AN ABSTRACT OF THE THESIS OF

Kathleen Patricia Barton   for the degree of Master of Science

in Chemical Engineering   presented on   June 15, 1982

Title: Calcium Carbonate Scaling in a Deluged Dry Cooling System

Abstract approved: Redacted for Privacy

Dr. James G. Knudsen

Scaling characteristics of calcium carbonate on a heated surface in a deluged dry cooling system were investigated. Bulk temperature of the deluge water was maintained constant at 90°F. Air flow velocity was maintained constant at 181 cfm., and deluge water flow was maintained at the minimum level that provided thorough wetting on the heat transfer surface. The heat flow ranged from 540 Btu/hr-ft^2 to 1616 Btu/hr-ft^2. The wall temperatures ranged from 90°F with the deluge water on, to 120°F to 240°F with the deluge water off. Deluge water was supplied as city water fortified with dissolved calcium carbonate. The calcium hardness ranged from 144 ppm $CaCO_3$ to 177 ppm $CaCO_3$, and the pH ranged from 7.5 to 8.7. The deluge time ranged from 20 sec. to 8 min., and the drying time between deluges was maintained constant at 10 min.

The amount of scale deposited on the horizontal cylindrical surface was a function of the radial position, with the greatest amount of fouling occurring at the bottom. The rate of growth of scale was a function of water chemistry, pH, number of deluge cycles, and duration of deluge cycle. The fouling resistances after 1500 cycles ranged from 0.2 x 10^{-4} hr-ft^2-°F/Btu for Langelier

Saturation Index (LSI) of -1.2 to 1.3 x 10^{-4} hr-ft^2-°F/Btu for LSI of 1.0. The net deposition was dependent on both sensible and evaporative heat transfer effects. The deposition rate was constant for the first 1500 cycles, and it declined after that. The amount of data was insufficient to allow determination of the cause for the decline. It was not determined whether the fouling resistance had reached an asymptotic value. The heat flux appeared to have no effect on the fouling rate.

Calcium Carbonate Scaling In A
Deluged Dry Cooling System

by

Kathleen Patricia Barton

A THESIS

submitted to

Oregon State University

in partial fulfillment of
the requirements for the
degree of

Master of Science

Completed June 1982

Commencement June 1983

APPROVED:

Professor of Chemical Engineering
in charge of major

Chairman of Chemical Engineering Department

Dean of Graduate School

Date thesis is presented ___June 15, 1982___

Typed by Margi Wolski for ___Kathleen Patricia Barton___

ACKNOWLEDGEMENT

TABLE OF CONTENTS

Table of Contents, continued

LIST OF FIGURES

LIST OF TABLES

CALCIUM CARBONATE SCALING IN A
DELUGED DRY COOLING SYSTEM

I. INTRODUCTION

In a dry cooling tower system, waste heat is transferred from an intermediate fluid such as condensed steam to the air by means of an air-cooled heat exchanger. During the cooler periods of the year the cooling tower operates as a totally dry system. However, during warm periods the efficiency of the heat exchanger can be increased by deluging the heat exchanger surface with water. Besides reducing the air temperature, the sensible heat exchange to the air is augmented by evaporative heat transfer from the deluge water (14).

Of concern in the operation of a deluged dry cooling tower is the tendency of the deluge water to deposit dissolved solids on the heat transfer surface. Deposition can occur by two mechanisms (7):

1. Decreasing solubility of certain salts with increasing temperature, and

2. Deposition of dissolved solids due to evaporation of the fluid.

The deposition of calcium carbonate scale in a deluged dry cooling system was evaluated as a function of duration and number of deluge cycles, the temperatures of the deluge water and the scaling surface, and water composition and pH.

II. GENERAL INFORMATION: PRECIPITATION FOULING

Precipitation fouling has been defined by Hasson (7) as the deposition of a solid layer on a heat transfer surface. The deposit, or scale, is caused by precipitation of normal solubility salts onto a subcooled surface or inverse solubility salts onto a superheated surface (2,3). It can also be caused by supersaturation due to fluid evaporation. The scale can range from a hard, well-bonded crystalline structure to a loose, powdery "soft scale" (7).

Scale formation is a strong function of the heat flux, bulk water temperature, water chemistry, dissolved salt concentration, and fluid flow characteristics. Surface roughness (except for its influence on induction time), surface material, and surface geometry have much weaker influence on scale formation (15).

Mechanisms of Fouling

Hasson (7) states that the primary driving force in precipitation fouling is the supersaturation level of the depositing species. Supersaturation can occur by concentration change due to evaporation. Alternatively, for the case of inverse solubility carbonates, the solubility decreases with increase in temperature.

The crystallization reactions for the formation of calcium carbonate are:

$$2HCO_3^- \rightleftharpoons CO_3^{-2} + H_2O + CO_2 \uparrow \qquad \text{Eqn. (1)}$$

$$Ca^{+2} + CO_3^{-2} \rightleftharpoons CaCO_3(s) \qquad \text{Eqn. (2)}$$
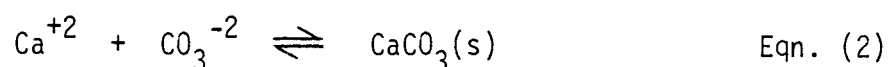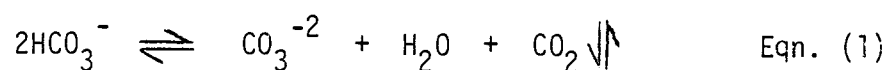
Carbon dioxide exists in water as bicarbonate ion, thus the concentration of calcium carbonate is dependent on the level of dissolved carbon dioxide gas in the liquid. When supersaturation occurs, the bicarbonate ion decomposes, forming CO_3^{-2} and releasing CO_2 (3). The carbonate concentration is also dependent on the pH of the system, since the form of the carbon species in water as molecular CO_2, HCO_3^-, or CO_3^{-2} depends on pH. High pH favors CO_3^{-2} (5).

The saturation concentration is determined by the solubility product

$$[Ca^{+2}]s[CO_3^{-2}]s \equiv K'sp \qquad \text{Eqn. (3)}$$

Thus, precipitation occurs when the water becomes supersaturated with calcium ion.

$$[Ca^{+2}] > [Ca^{+2}]s \equiv K'sp/[CO_3^{-2}]s \qquad \text{Eqn. (4)}$$

A widely used index for predicting the calcium carbonate scale forming tendency is the Langelier Index, LSI. It is described in detail in Appendix C. A positive value of LSI indicates that the water is supersaturated and precipitation can occur.

Rate of Fouling

The net accumulation of scale is a combination of delay time, deposition, aging, and re-entrainment.

Delay Time

The delay time is defined as the time required for initial deposition to occur. The delay time depends on the probability that a

particle that is transported to the surface or that forms at the surface will stick to the surface. Thus, it is a function of the adhesion of the particle, the residence time of the particle, and the surface conditions (10). Generally, delay times have been observed to be shorter for surfaces that are rough than for smooth surfaces and for surfaces that have been fouled and then cleaned than for new surfaces. However, the delay time does not seem to affect the shape of the subsequent deposition rate curve (10).

Deposition

Hasson (7) and Somerscales (18) describe the mechanisms that act together to govern scale deposition:

1. Nucleation processes in the body of the fluid and at the heat transfer surface;

2. Transport to the surface;

3. Attachment and subsequent formation of the deposit.

Somerscales (18) summarized the rate of formation, $\dot{m}_d$, of the fouling material for evaporation and sensible heat scaling of saturated solutions:

$$\dot{m}_d = \frac{C_b - C_s}{\frac{1}{k_m} + \frac{1}{k_r}} \qquad \text{Eqn. (5)}$$

where k_m is the mass transfer coefficient and k_r is the first order reaction rate constant. This is equivalent to the Reitzer model noted by Epstein (2). Another model proposed by Epstein is (3):

$$\dot{m}_d = \frac{C_b - C_{sat}}{\frac{1}{k_m} + \frac{1}{k_r}(C_s - C_{sat})^{n-1}} \qquad \text{Eqn. (6)}$$

At high fluid velocities, surface attachment controls, and $C_b \sim C_s$, so (3)

$$\dot{m}_d = k_r(C_b - C_{sat})^n \qquad \text{Eqn. (7)}$$

An alternate form of the last equation is that of Taborek et al. (19):

$$\dot{m}_d = C_0 P_d(\Omega)^n \exp\left[\frac{-E}{R_g T_s}\right] \qquad \text{Eqn. (8)}$$

where $k_r = C_0 \exp\left[\frac{-E}{R_g T_s}\right]$, is a parameter characterizing the fluid and its supersaturation potential, and P_d is a sticking probability.

However, at low fluid velocities, mass transfer controls (3),

$$\frac{1}{k_m} \gg \frac{1}{k_r} \qquad \text{and} \qquad \dot{m}_d = k_m(C_b - C_{sat}) \qquad \text{Eqn. (9)}$$

$$\text{or} \qquad \dot{m}_d = C_1 P_d(\Omega) \qquad \text{Eqn. (10)}$$

In this case then, the deposition rate is directly proportional to the mass transfer coefficient, the sticking probability, and a concentration gradient.

In the case of a deluged dry cooling tower, both evaporation and sensible heat precipitation may occur, and there can be two process conditions leading to supersaturation (7):

1. Deluge water containing an inverse solubility salt is heated above its solubility limit;

2. Evaporation causes deluge water containing a dissolved salt to become supersaturated.

Although the first condition can occur in the bulk, the bulk temperature of the deluge water is generally too low and the precipitation from heating probably occurs at or near the heat transfer surface.

Using Epstein's model to represent the deluge condition #1 for regions of complete wetting of exchanger surface, if the deluge flow rate is low:

$$\dot{m}_d = k_m(C_b - C_{sat}) \qquad \text{Eqn. (9)}$$

and if the deluge flow rate is high,

$$\dot{m}_d = k_r(C_b - C_{sat})^n \qquad \text{Eqn. (7)}$$

Condition #2, evaporation, occurs after the deluge water is shut off. Gardner (6) studied drainage and evaporation of a liquid film on a horizontal cylindrical surface. According to his analysis, there are two stages in the evaporation process: drainage and actual evaporation. If the heat flux is very high, then evaporation will always dominate and the total amount of deposition is independent of the location on the cylinder. Otherwise, the rate of film thinning is dependent on both evaporation and drainage, and the evaporation does not become dominant until the film is sufficiently thin. Assuming a laminar film around the cylinder, the fluid will drain such that the film thickness increases with distance, y, from the top of the cylinder as shown:
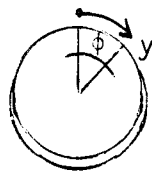
Gardner shows that the total mass deposited following deluge is directly proportional to the film thickness and therefore to y.

The second stage of the process is termed "dryout." At the edges of the film layer, the film thickness becomes sufficiently small so that the evaporation rate becomes dominant. During dryout the remaining particulates and salts are deposited at the surface.

Gardner also shows that the diffusivity of the salt has minimal influence upon the total amount of salt deposited, i.e., a salt of high diffusivity will still deposit in proportion to y.

Removal

Under certain flow conditions, the deposit that has been formed on the heat transfer surface can be sheared off. The various re-entrainment flux models are summarized by Epstein (2, 4). The most widely accepted model assumes the removal rate to be directly pro-portional to the accumulated deposit mass, m:

$$\dot{m}_r = b_1 m \qquad \text{Eqn. (11)}$$

Taborek et al. (11) proposed that the removal flux is proportional to both the fluid velocity and shear, and the accumulated deposit thickness, x_f:

$$\dot{m}_r = b_2 \frac{\tau}{\psi} x_f = B \frac{\tau}{\psi} m \qquad \text{Eqn. (12)}$$

Aging

As soon as the scale deposits on the heat transfer surface it begins to age. The aging process can either weaken or strengthen the

structure. In general, in cases of constant heat flux and increasing deposit temperature during the drying period after deluge, the inverse solubility deposit may increase in strength (3).

Net Rate of Deposition

For either of the removal models, when there is re-entrainment, the net accumulation of scale becomes:

$$\frac{dm}{d\theta} = \dot{m}_d - \dot{m}_r \qquad \text{Eqn. (13)}$$

For an evaporating solution there is no removal term and the equation becomes the deposition equation:

$$\frac{dm}{d\theta} = \dot{m}_d = K(C_b - C_{sat})^n \qquad \text{Eqn. (14)}$$

where $n = 1$ for a non-stirred evaporating liquid (2).

However, under deluge conditions, the removal term will depend on the flow characteristics of the deluge water and the adhesion of the deposit.

Epstein (3) has recently proposed that asymptotic deposition can occur even when there is no re-entrainment, because of various auto-retardation mechanisms. In these cases,

$$\frac{dm}{d\theta} = \dot{m}_d - \dot{m}_r \qquad \text{Eqn. (13)}$$

where

$$\dot{m}_d = K(C_b - C_{sat})^n \qquad \text{Eqn. (14)}$$

Sensible Heat Fouling

For sensible heat fouling of saturated solutions at constant heat flux, n = 1 (2, 5). Then,

$$\dot{m}_d = K(C_b - C_{sat}) = \text{constant} \qquad \text{Eqn. (15)}$$

where $K = k_r$ for high fluid velocity and $K = k_m$ for low fluid velocity. The removal rate is

$$\dot{m}_r = B \frac{\tau}{\psi} m \qquad \text{Eqn. (12)}$$

Integration of Eqn. (13) gives the Kern-Seaton equation (13)

$$m = m^*[1-\exp(-\theta/\theta_c)] \qquad \text{Eqn. (16)}$$

The quantity $m^* = \dot{m}_d \theta_c$ represents the asymptotic fouling deposit and θ_c is the time required to reach asymptotic fouling. The time constant, θ_c, does not include the delay time.

Evaporation Fouling

The situation of heat transfer via evaporation to dryness of a liquid film is the most conducive of all fouling conditions. For an evaporating solution that is saturated in the bulk and supersaturated at the surface with respect to the scaling species,

$$\frac{dm}{d\theta} = K(C_b - C_s) = \text{constant} \qquad \text{Eqn. (17)}$$

Integrating:

$$m = K_1 \theta \qquad \text{Eqn. (18)}$$

In this case the net deposit increases linearly with time, and there is no asymptote.

Fouling Resistance

The unit thermal fouling resistance, R_f, is related to the amount of scale deposited on the heat transfer surface by (2)

$$R_f = \frac{m}{\rho_f k_f} \qquad \text{Eqn. (19)}$$

where ρ_f and k_f are the density and thermal conductivity of the deposit. The fouling rate, then, is defined as

$$\frac{dR_f}{d\theta} = \frac{1}{\rho_f k_f} \frac{dm}{d\theta} \qquad \text{Eqn. (20)}$$

assuming $\rho_f k_f$ is constant. Substitution into Equation (13) gives (18, 10)

$$\frac{dR_f}{d\theta} = \phi_d - \phi_r \qquad \text{Eqn. (21)}$$

where ϕ_d and ϕ_r are the deposition and removal fouling rates and

$$\phi_d = C_2 \dot{m}_d$$

$$\phi_r = C_3 \dot{m}_r$$

For pure evaporation with no re-entrainment, and using the previously developed equation for $\dot{m}_d$, the fouling resistance is given by

$$R_f = C_4 \theta \qquad \text{Eqn. (22)}$$

During sensible heating deluge conditions, if re-entrainment or autoretardation effects exist, then

$$R_f = R_f *[1-\exp(-\theta/\theta_c)] \qquad \text{Eqn. (23)}$$

where R_f^* is the asymptotic fouling resistance and θ_c is the time constant.

Measurement of Fouling Resistance

The fouling resistance can be determined for a heat transfer surface from the fundamental equation for the overall heat transfer coefficient (11):

$$R_f = \frac{1}{U_f} - \frac{1}{U_o} - \frac{1}{h_f} + \frac{1}{h_o} \qquad \text{Eqn. (24)}$$

where U_o is the initial heat transfer coefficient for the clean surface,

$$\frac{1}{U_o} = \frac{1}{h_o} + R_w = \frac{T_{wo} - T_{bo}}{q/A} \qquad \text{Eqn. (25)}$$

and U_f is the heat transfer coefficient at time θ after fouling;

$$\frac{1}{U_f} = \frac{1}{h_f} + R_f + R_w = \frac{T_w - T_b}{q/A} \qquad \text{Eqn. (26)}$$

$h_o, h_f \equiv$ bulk fluid heat transfer coefficient

$R_w \equiv$ thermal resistance of tube material

$T_{wo}, T_w \equiv$ local wall temperature

$T_{bo}, T_b \equiv$ local bulk temperature

$q/A \equiv$ heat flux per unit area

These terms are illustrated in Figure 1.

For cases of constant heat flux, constant (or zero) flow velocity, constant h, and constant bulk temperature, the deposit surface temperature will remain constant. Then, at any particular time θ,

$$R_f = \frac{1}{q/A} [\Delta T_f - \Delta T_c] = \frac{\Delta T}{q/A} \qquad \text{Eqn. (27)}$$

and ΔT is the temperature driving force for fouling.

Any measured deviation from this linear relationship could be caused by re-entrainment or autoretardation effects.
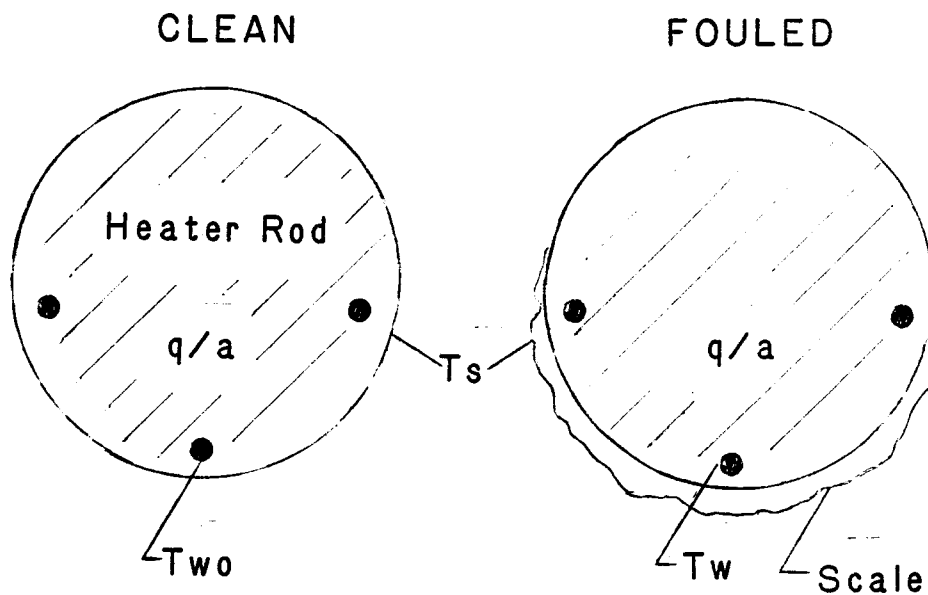
Figure 1. Definition of terms for measurement of R_f

III. EXPERIMENTAL EQUIPMENT

The experimental equipment consisted of three sections: the deluge water supply, the simulated deluge cooling unit, and the measurement test section.

Deluge Water Supply

The deluge water was supplied from the basin makeup water used by Knudsen and Roy (16) for their experiments. Therefore water chemistry, pH, and percent solids were governed by those other experiments.

The data for the makeup water is given in Appendix C. As described in previous works of Coates (1), the makeup water composition was maintained by adding fortified city water to recycled cooling tower water.

The deluge cooling water was pumped from the basin and recycled back to the basin after deluge.

Deluge Cooling Unit

A diagram of the experimental cooling tower unit is shown in Figure 2.

The cooling tower shell was made of plexiglass, dimensions $0.96 \times 0.96 \times 4.88$ ft^3. It was totally enclosed except for a hole at the top where the blower was mounted, and a drainspout at the bottom to allow drainage of the deluge water.

A heating rod was used to simulate a single-pass heat exchanger.
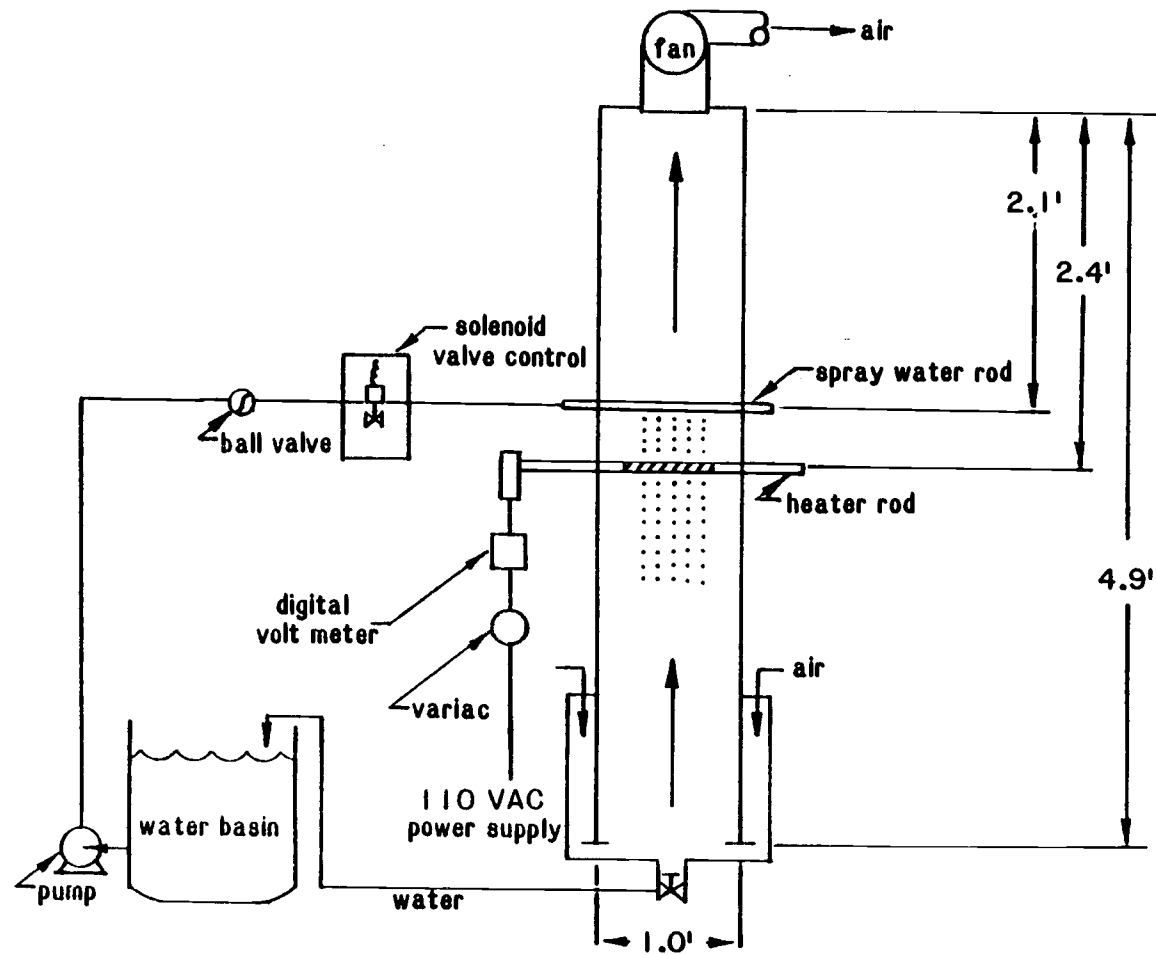
Figure 2. Schematic Flow Diagram of Experimental Equipment

It was mounted horizontally 2.46 ft from the bottom of the tower. The rod is made of Admiralty brass, with specifications shown in Figure 3. It has a 22.0 ohm electric resistance heater embedded in a section 6.0 in. long which provides the desired heat flux.

Three chromel-constantin (Type E) thermocouples are located just underneath the surface and approximately 2.0 inches in from one edge of the heater. Knowledge of the thermal conductivity of the metal and the location of the thermocouples from the surface enable calculation of the heated surface temperatures. The values of k/x for the three thermocouples are given in Figure 3.

A fourth thermocouple, which is a bulk probe, was used to measure the wet and dry bulb air temperatures at the locations indicated in Figure i of Appendix E and to measure the deluge water temperature.

The electric power to the heater was regulated through a 115 volt 5 amp variac and measured with a Micronta digital voltmeter.

The air flow through the tower was provided by an induced draft EG&G Rotron blower mounted at the top of the tower. The flow rate was chosen to be the maximum allowable air flow without causing liquid water to be drawn up and out of the tower. This rate was measured to be 180.8 cfm ± 1.8 cfm.

The deluge water was sprayed from a 3/8-inch o.d. copper tube mounted horizontally 4.0 in. above the heated rod. The water was sprayed through 14, 1/32-in. holes each 0.5 in. apart, located on the bottom of the tube. The flow rate of the water spray was adjusted and held with a ball valve such that a continuous liquid flow was provided on the heated rod during the deluge period. Although the
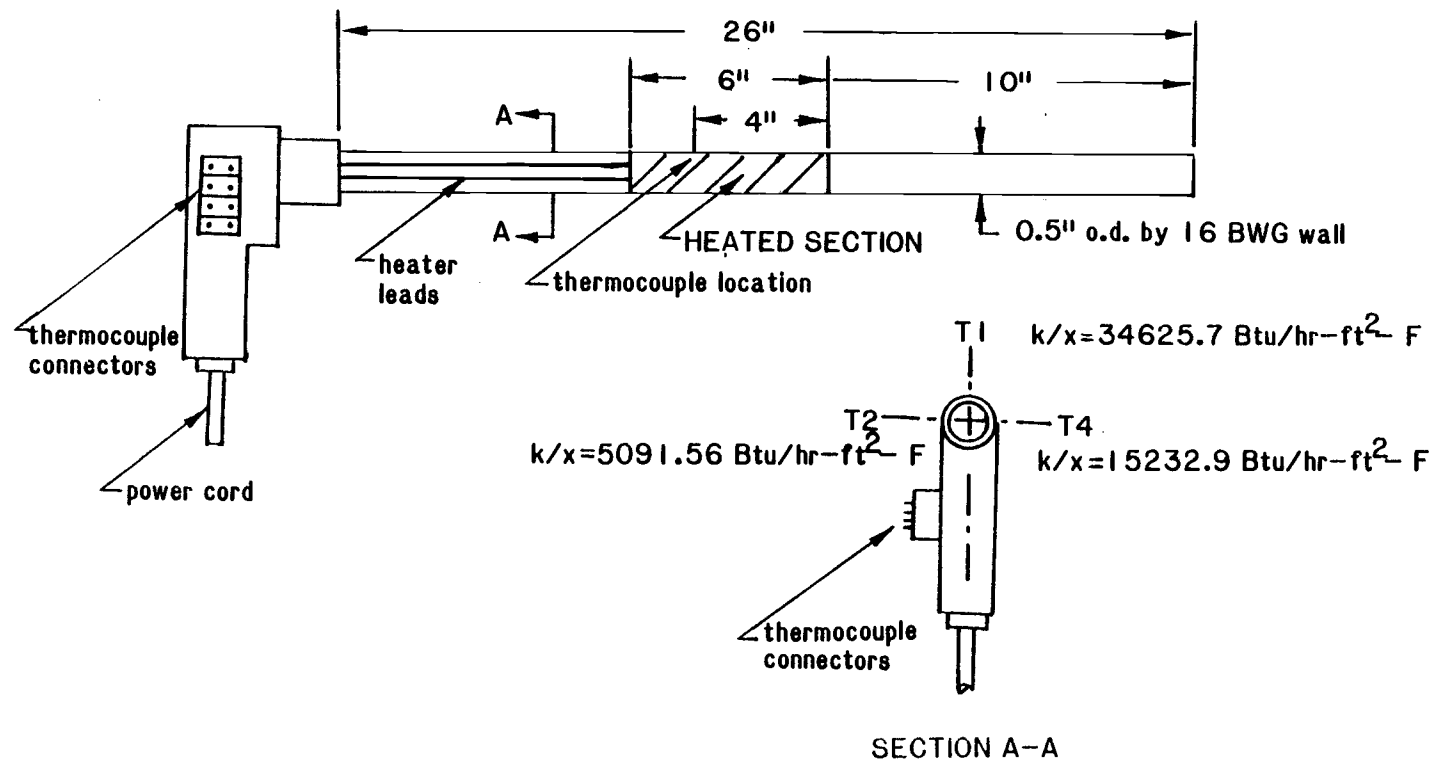
Figure 3. Heater Rod--Heated Section and Thermocouple Locations

flow rate was kept low in order to simulate a deluge cooling tower situation, i.e. water cascading onto the heat transfer surface, no effort was made to control the flow rate to a specific precision.

There were two contolled parameters in the deluge cycle, the duration of deluge, and the dry interval between each deluge. The deluge cycle was maintained by a control unit connected to the water supply via an on-off solenoid valve. The cycle time could be set for any increment of 20.0 sec. from 20.0 to 255.0 sec. $\pm$ 0.2 sec., and the duration time could be set for any increment of 20.0 sec. from 20.0 to 255.0 sec. $\pm$ 0.2 sec. The cycle was repeated until the desired number of cycles was reached and the unit was manually shut off. In addition, the unit could be operated manually.

The piping for the water supply and return was made of 1.0 in. o.d. CPVC (chlorinated polyvinyl chloride). One-half inch teflon tubing was used to connect the deluge cycle controller to the water supply on one side and to the copper spray tube on the other side of the control valve. All fittings were brass.

Measurement Test Section

The critical part of the experiment is the ability to accurately measure the desired parameter, the fouling resistance. It is particularly difficult to measure R_f on-line in a deluge dry cooling tower for two reasons:

1) For each cycle, the system changes from totally wetted surface to evaporating film surface to dry surface, thus the surface temperature depends on the state of the

system, and;

2) The bulk temperature can be defined as either the wet or dry bulb temperature of the inlet, inside, or exit air. This is a problem not only because it is a function of the room conditions, but also because the heat transfer coefficient, h_a, of air is low relative to $1/R_f$ and therefore $1/h_a$ is very high. Thus, for $h_a \simeq 10$ Btu/hr - ft^2 - °F, an error of $\pm$ 0.5% will mask R_f. It was also decided that the deluge water temperature is a poor choice of bulk medium because the cooling is actually provided by a combination of air flow and deluge water, and the ΔT between deluge water and heated surface is too small to provide the necessary measurement accuracy.

A discussion of the above is given in Appendix E. For the reasons stated, the measurements of fouling resistance were made in the Calibration Test Unit developed by Knudsen and in use in the Oregon State University Chemical Engineering Building. A diagram of that unit is shown in Figure 4. For measuring purposes, water flow rate and heat flux were held constant at 4.474 gpm and 2.8441 x 10^4 Btu/ hr-ft^2, respectively. The bulk water was provided from a storage tank, and its temperature varied from 66.0 $\pm$ 10.0 °F.

There was no observed scale removal during the process of moving the heater rod from experimental apparatus to measurement apparatus, nor from the measurement process itself.
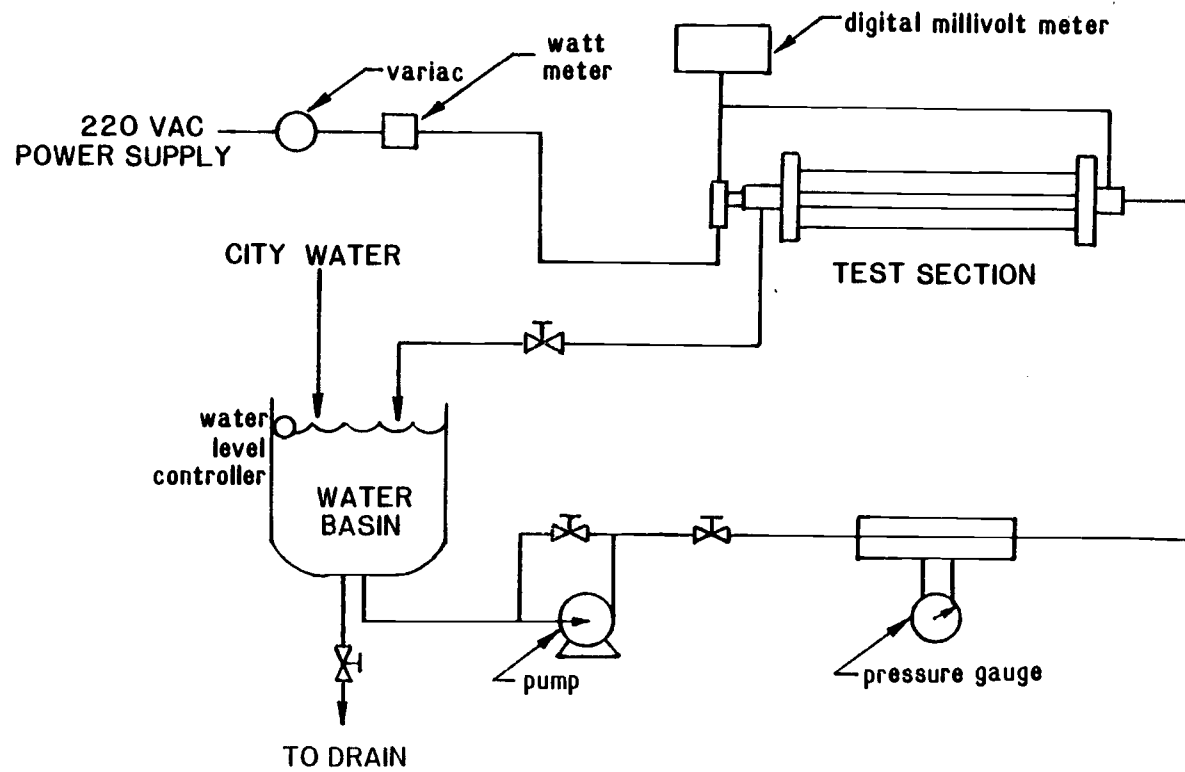
Figure 4. Calibration Test Unit

IV. EXPERIMENTAL PROCEDURE

The objectives of the experiment were:

1. To determine the scaling characteristics of cooling tower water on a heated surface that is periodically wetted;

2. To determine the effect of the duration of the deluge on the induction time and the net rate of fouling.

An experimental run consisted of 2500-3000 deluge cycles of fixed duration and interval. Twenty-five hundred cycles were considered to be typical of 7-10 years of operation of a deluge dry cooling tower. Temperature measurements were recorded daily, and visual observations were noted.

Runs 1, 2, and 3 were of 2 minutes, 8 minutes, and 1/3 minute deluge duration, respectively, and were all of equal drying interval. For these runs, air flow rate, water flow rate, water temperature, and heat flux were maintained constant. Because nucleation and deposition for evaporation fouling on a horizontal cylinder are dependent on the radial surface position, the positions of the thermocouples relative to the top of the rod were the same for all runs after Run 1 when T1 was moved to the bottom of the rod.

Run 4 was of 1 minute deluge duration. Air flow rate, water flow rate, and water temperature were constant and were equal to the values for Runs 1, 2, and 3. The heat flux was increased by 3x from the previous runs.

The deluge water was supplied from the makeup water of Roy (16). Therefore, the water quality was not maintained constant for all the runs. The pH varied from 7.5 to 8.7 and the calcium hardness varied from 140 ppm to 200 ppm.

V. CALCULATION PROCEDURES

As previously explained, all measurements for fouling resistance calculations, except for Run 1, were taken in the Calibration Test Unit. Separate initial conditions were calculated for each run.

Calculation of Initial Conditions

The initial overall heat transfer coefficient, U_o, bulk fluid heat transfer coefficient, h_o, and wall resistance, R_w, are related by the following equation:

$$\frac{1}{U_o} = \frac{1}{h_o} + R_w \qquad\qquad \text{Eqn. (25)}$$

where

$$\frac{1}{U_o} = \frac{T_{wo} - T_{bo}}{q/A}$$

$$R_w = x/k$$

$$\frac{1}{h_o} = \frac{T_{so} - T_{bo}}{q/A}$$

and the measured parameters are:

T_{wo} = local wall (thermocouple) temperature, °F

T_{bo} = local bulk temperature, °F

q/A = heat flux per unit area, Btu/hr-ft^2-°F

x/k = thermal resistance of tube material, ft^2-hr-°F/Btu

The local surface temperature, T_{so}, can also be calculated.

Calculation of Fouled Conditions

For constant heat flux and flow velocity, the fouling resistance, R_f, can be calculated by

$$\frac{1}{U_f} = \frac{1}{h_f} + R_w + R_f \qquad\qquad \text{Eqn. (26)}$$

where

$$\frac{1}{U_f} = \frac{T_w - T_b}{q/A} \equiv \quad \begin{array}{l}\text{overall heat transfer}\\\text{resistance at the fouled}\\\text{conditions}\end{array}$$

$$\frac{1}{h_f} = \frac{T_s - T_b}{q/A} \equiv \quad \begin{array}{l}\text{bulk fluid heat transfer}\\\text{resistance at the fouled}\\\text{conditions}\end{array}$$

Subtracting Eqn. (25) from Eqn. (26);

$$R_f = \frac{1}{U_f} - \frac{1}{U_0} - \frac{1}{h_f} + \frac{1}{h_0} \qquad\qquad \text{Eqn. (24)}$$

and the fouling resistance can be calculated from knowledge of initial and fouled conditions.

Calculation of h_f

If the bulk fluid temperature is constant for all measurements, then $h_0 = h_f$. Otherwise, h_0 and h_f can be related according to the following equation (12):

$$h = 150(1+0.011T_b)(V')^{0.8}/(D')^{0.2} \qquad\qquad \text{Eqn. (28)}$$

$V' \equiv$ average velocity

$D' \equiv$ diameter of tube

For constant V', D':

$$\frac{h_o}{h_f} = \frac{1+0.011T_{bo}}{1+0.011T_b}$$

Then, Eqn. (30) can be written as

$$R_f = \frac{1}{U_f} - \frac{1}{U_o} - \frac{1}{h_o} \; [(\frac{1+0.011T_{bo}}{1+0.011T_b}) - 1] \quad \text{Eqn. (29)}$$

A comparison of predicted R_f vs. T_b for measured $(T_w - T_b)$ at the conclusion of Run #4 is shown in Table 2 of Appendix E. The empirical equation gives reasonable correlation to the reference R_f at T_{bo}, and the scatter is actually within experimental error for R_f measurement.

Calculation of Error

If R_f is a function of the independent variables m_1, m_2, m_3, ... m_n,

$$R_f = R_f(m_1, m_2, m_3, ... m_n)$$

and S_1, S_2, S_3,... S_n are the uncertainties in the independent variables, then the total uncertainty S_R is given by the equation (8):

$$S_R = [(\frac{\partial R}{\partial m_1} S_1)^2 + (\frac{\partial R}{\partial m_2} S_2)^2 + ... + (\frac{\partial R}{\partial m_n} S_n)^2]^{\frac{1}{2}} \quad \text{Eqn. (30)}$$

Equation (29) can be rewritten as:

$$R_f = \frac{T_w - T_b}{q/A} - \frac{T_{wo} - T_{bo}}{q/A} -$$

$$0.011 \; (\frac{T_{wo} - T_{bo}}{q/A} - \frac{x}{k})(\frac{T_{bo} - T_b}{1+.011T_b}) \quad \text{Eqn. (31)}$$

$$R_f = R_f(T_w, T_b, T_{wo}, T_{bo}, q/A)$$

$$\frac{\partial R_f}{\partial T_w} = \frac{1}{q/A}$$

$$\frac{\partial R_f}{\partial T_b} = \frac{1}{q/A} + \frac{.011(1+.011T_{bo})}{(1+.011T_b)^2} \left[\frac{T_{wo}-T_{bo}}{q/A} - \frac{x}{k} \right]$$

$$\frac{\partial R_f}{\partial T_{wo}} = \frac{-(1+.011T_{bo})}{q/A(1+.011T_b)}$$

$$\frac{\partial R_f}{\partial T_{bo}} - \frac{1}{q/A} + \frac{.011}{(1+.011T_b)} \left[\frac{2T_{bo}-T_b-T_{wo}}{q/A} + \frac{x}{k} \right]$$

$$\frac{\partial R_f}{\partial (q/A)} = \frac{f(T_w, T_b, T_{wo}, T_{bo})}{(q/A)^2}$$

The denominator of $\partial R_f/\partial(q/A)$ is very large compared with the other terms, and therefore $\partial R_f/\partial(q/A)$ is negligible compared with the other error terms. Representative values for T_{wo}, T_{bo}, T_w, T_b, and q/A and for S_n are given in Table 1. Values for S_n are based on the estimated precision of the instruments and measuring techniques.

From Equation (30) and Table 1, the maximum error is estimated to be:

$$S_R \simeq 0.00001419 \qquad hr\text{-}ft^2\text{-}°F/BTU$$

For (typical)

$$R_f \simeq 0.00003000 \qquad hr\text{-}ft^2\text{-}°F/BTU$$

Max. Relative Error = 47%

TABLE 1

ERROR CALCULATION

Variable, m	Measured Units	m_{avg}	Uncertainty, S_n
T_b, T_{bo}	°F	68.00	0.0311
T_w, T_{wo}	°F	113.0	0.290
q/A	Btu/hr-ft^2	28441.	284.41

VI. RESULTS AND DISCUSSION

The test conditions for each experimental run are summarized
in Table 2. The data for the individual runs and for the water
quality are included in Appendices E and C, and comparisons of foul-
ing resistance, R_f, as a function of number of deluge cycles for the
first three runs are shown in Figures 5, 6, and 7.

TABLE 2
EXPERIMENTAL RUN CONDITIONS

Run	Total Number of Cycles	Drying Interval, min.	Deluge Duration, min.	$(q/A)_{avg}$ Btu/hr-ft^2	Water Quality pH	ppm CaCO$_3$	LSI
1	2925	10.0	2.0	550.2	8.7	175	1.4
2	2500	10.0	8.0	539.8	8.5	144	1.0
3	3100	10.0	1/3	581.7	7.5	170	-0.6
4	2520	10.0	1.0	1616.0	7.5	177	-1.2

Results

Experimental Run 1

For this run the heated rod was mounted such that the three
thermocouples were positioned at the top and sides of the rod as
shown:

T_3

T_4(front), T_2(back)

|←2"→|

|← 6" →|

Bottom of Column
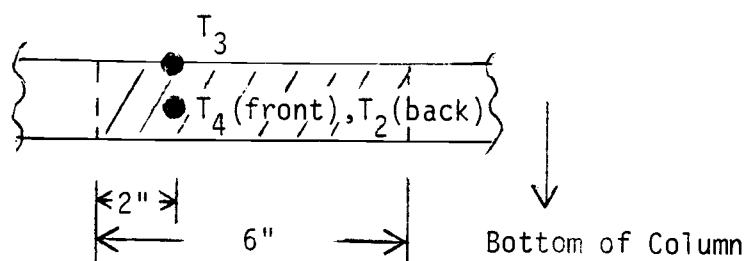
The data were widely scattered due to the error in T_b discussed in Appendix E. Qualitatively, It appears that the net fouling re-sistances at T_2 and T_4 increased linearly from 1000 to 1400 cycles. Then they decreased and eventually became constant.

The magnitude of the fouling resistance is expected to be a function of the position of the thermocouple relative to the bottom of the heated surface. This is due to the observation that the scale deposits first at the bottom of the rod.

Additionally, it was observed that due to drainage, the liquid film receded very quickly after the deluge cycle into liquid pools which were localized on the bottom of the cylinder as shown:
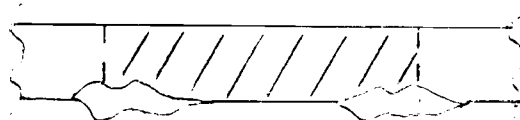
The pools seemed to locate in the same positions after each deluge. After the initial nucleation the scale deposit propagated from the original nucleation sites. It was also observed that the deposit thickness seemed to be greatest at the edges of the liquid pool
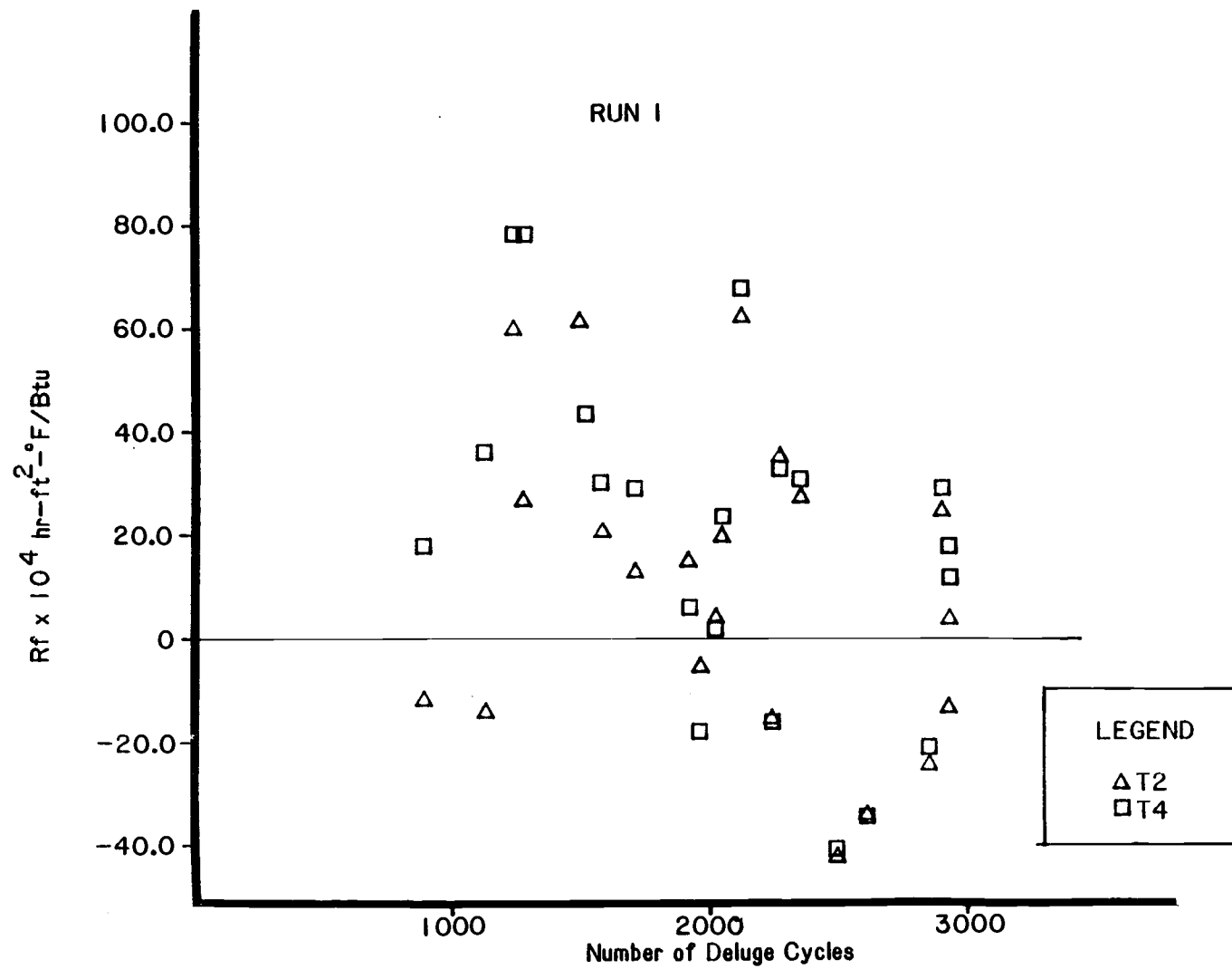
Figure 5. Fouling Resistance vs. Number of Cycles, Run 1
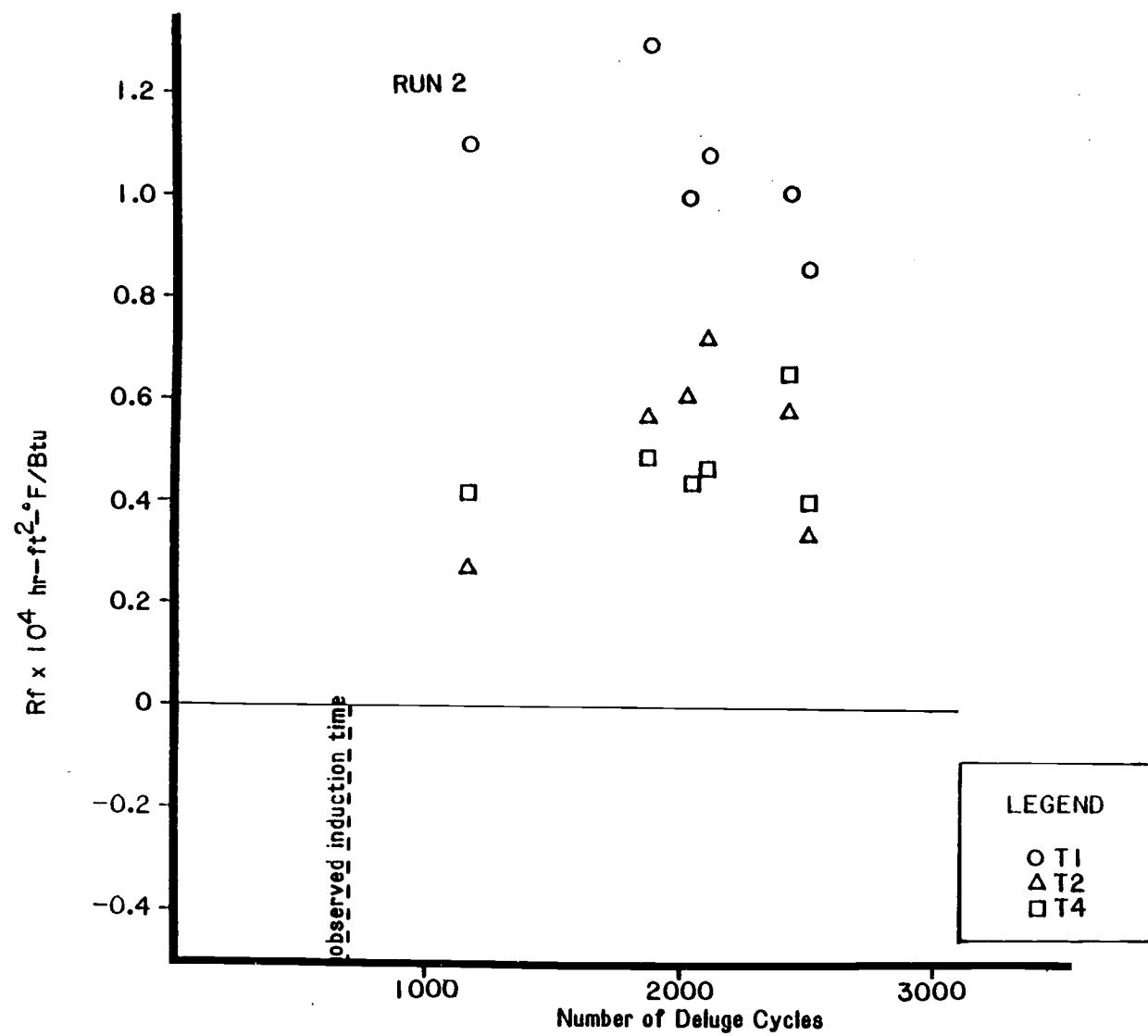
Figure 6. Fouling Resistance vs. Number of Cycles, Run 2
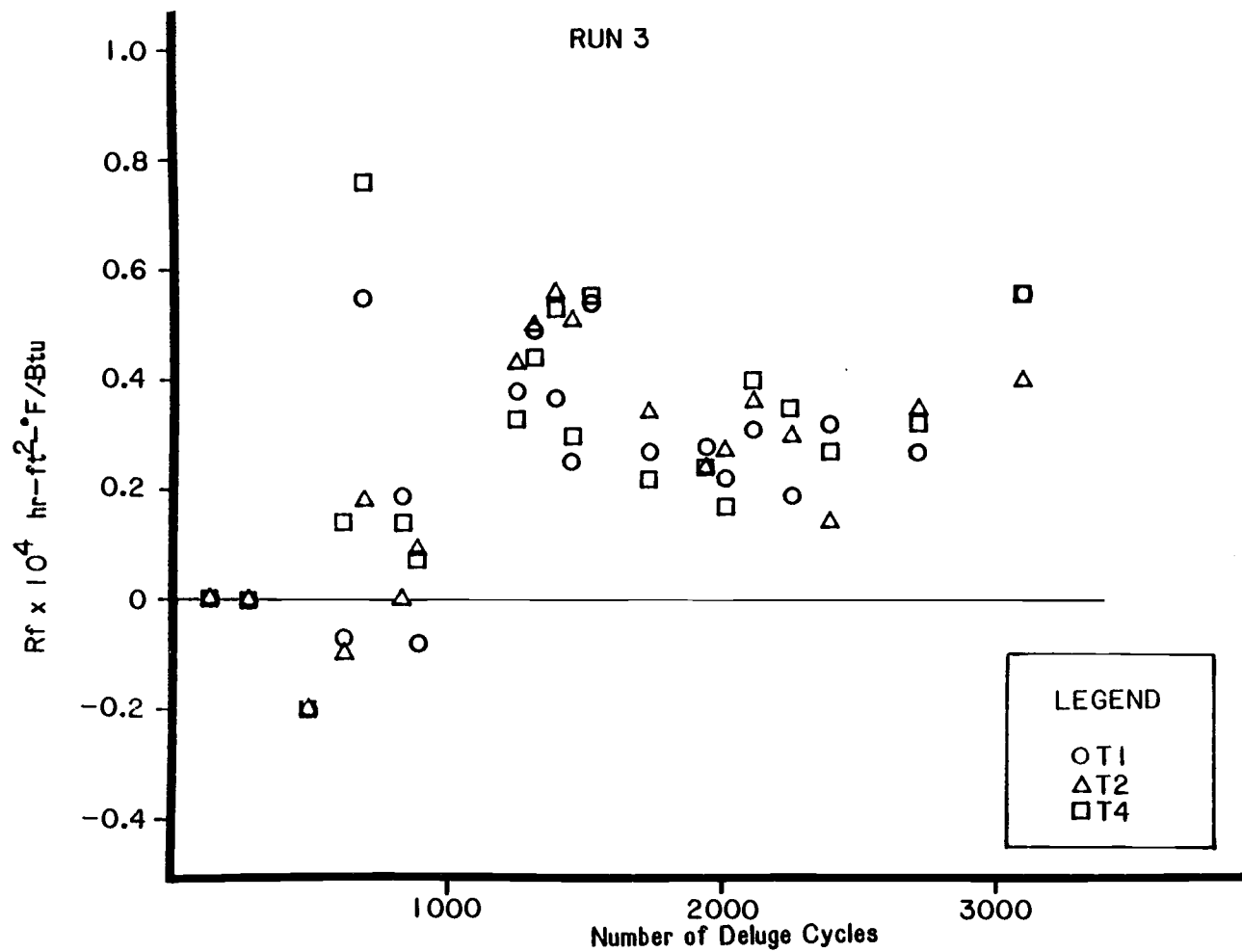
Figure 7. Fouling Resistance vs. Number of Cycles, Run 3

locations. This may be a result of a local concentration driving force at the initial dryout location. These observations agree with Gardner's analysis (8) which was discussed previously.

The scale was photographed macroscopically and microscopically at the end of the run. The micorgraphs are of scraped samples. These photographs are included in Figures 8, 9, and 10. The scale was hard, and although it looked as if it would flake off, it was very tenacious and could not be removed by rubbing or with a water wash.

Appendix C is a summary of the water chemistry data for the experimental runs. The average pH for Run 1 was 8.7 and the average calcium hardness was 175 ppm $CaCO_3$. The langelier Index was 1.4.

Experimental Run 2

Since it was observed during Run 1 that the scale propagated from drainage pools at the bottom of the heated cylinder, the thermocouples for this and subsequent runs were positioned such that thermocouple 1, T_1, was located at the bottom.
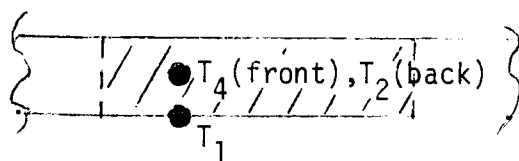
For the initial 1000 cycles of Run 2 the temperature measurements were taken in the experimental unit similarly to Run 1. It was then determined that the data scatter was unacceptable and the testing procedure was changed. The remaining measurements were taken in the Calibration Test Unit, and only the data after 1000 cycles are shown
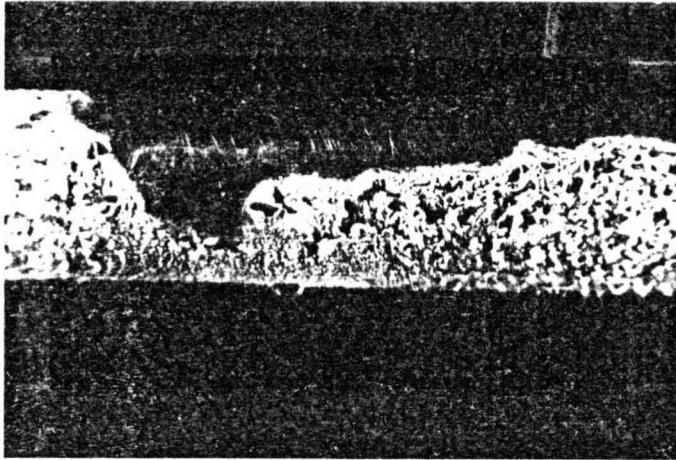
T4 at middle, r.h.s.
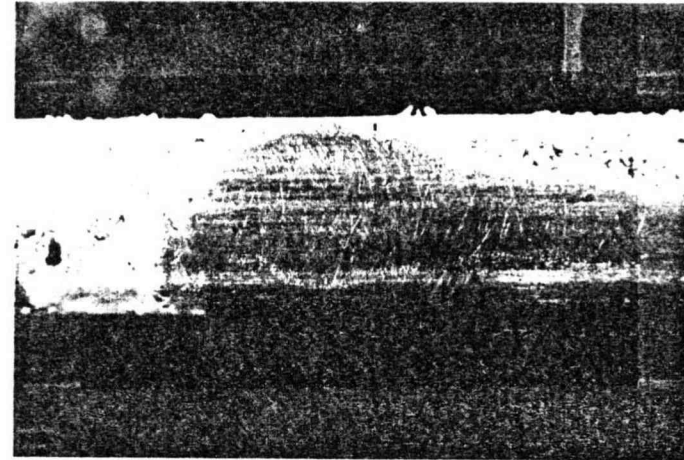
T2 at middle, r.h.s.
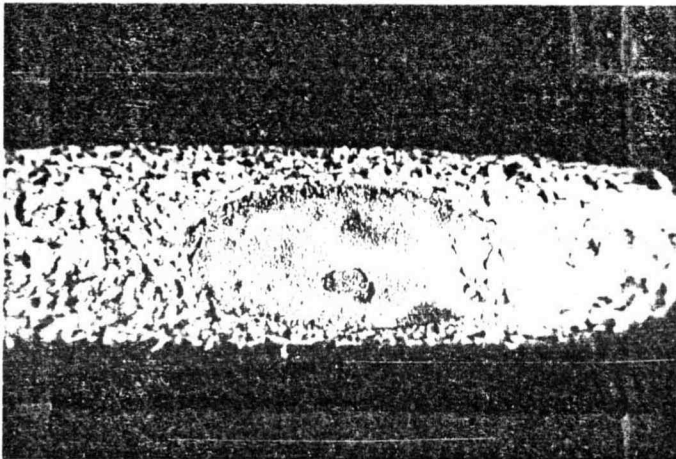
underside view
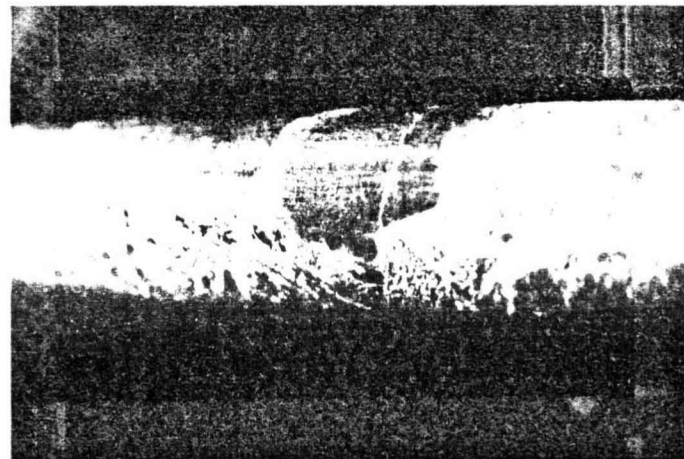
side view of swirl pattern

Figure 8. Photographs of Deposit on Heat Transfer Surface, Run 1.
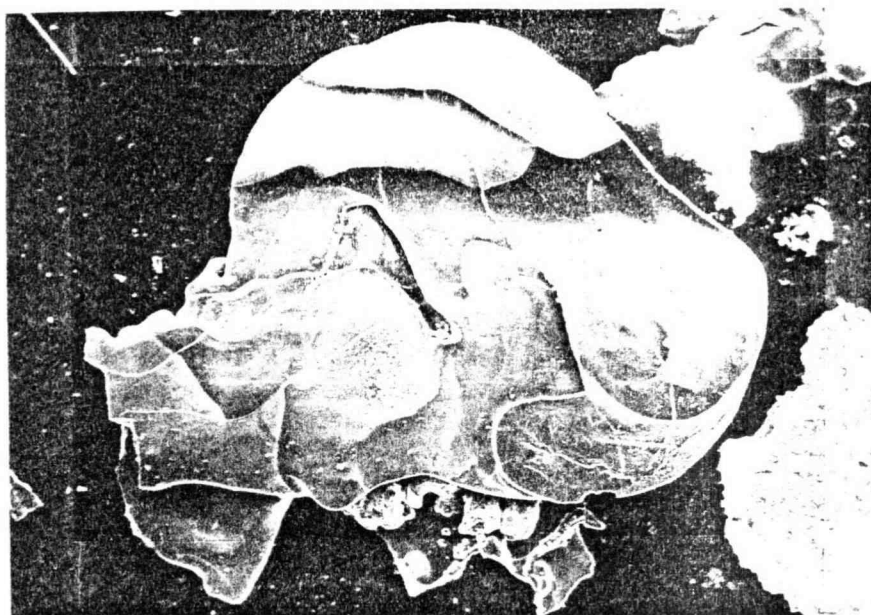
50x (#3080)
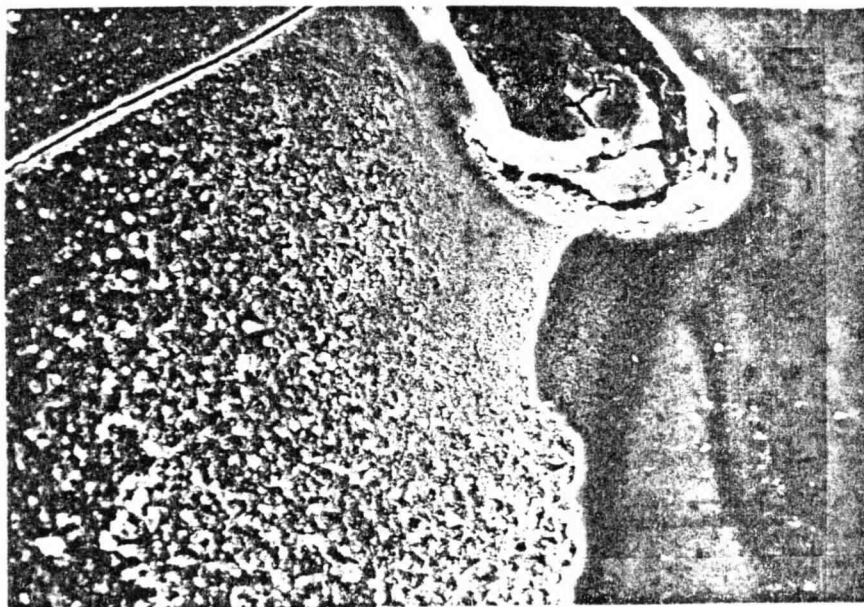
400x (#3081, centers into #3080)

Figure 9. SEM Micrographs of Deposit Particle from Run 1.
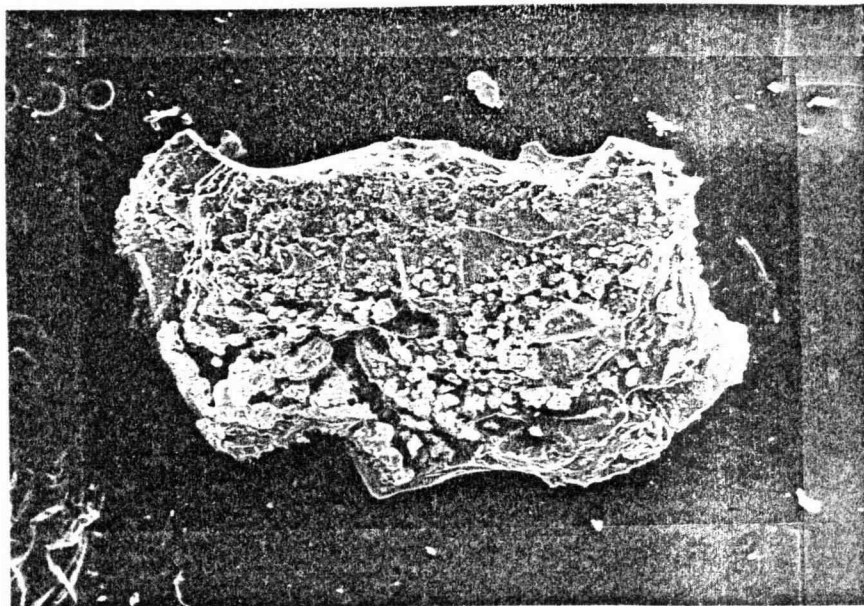
50x (#3084)
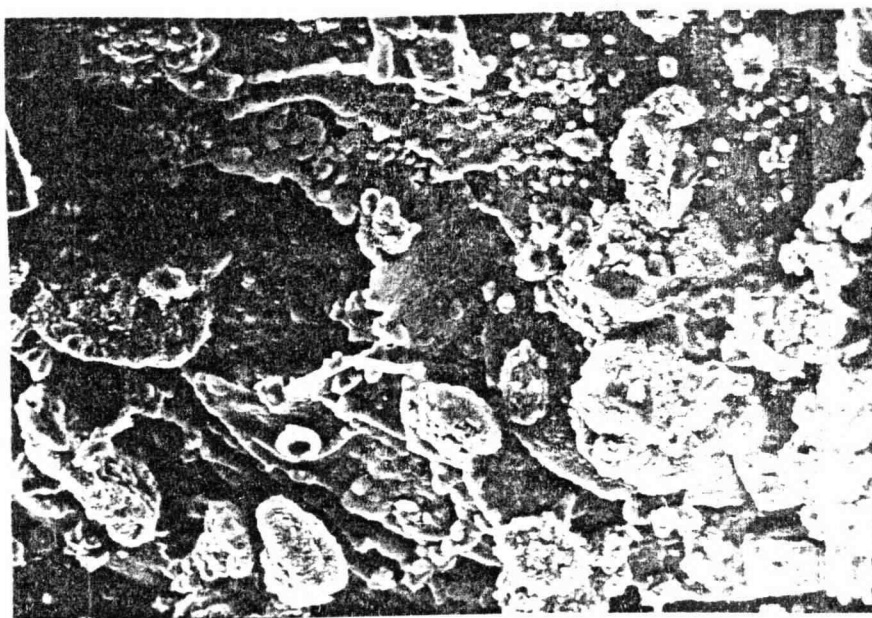
400x (#3085, centers into #3084)

Figure 10. SEM Micrographs of Deposit Particle from Run 1.

on Figure 7. The nucleation time at location T_4, the front center of the heated rod, was visually observed to be approximately 700 cycles. The nucleation times for T_1 and T_2 were detected from temperature measurements to be approximately 700 cycles also.

The fouling resistances for all thermocouple locations increased linearly after nucleation until approximately 2000 cycles. After that, there was a decline in the values of the fouling resistances.

The magnitude of the fouling resistances R_{f2} and R_{f4} were approximately equal, and the peak resistance was 0.6×10^{-4} hr-ft^2-°F/Btu. The magnitude of R_{f1} was greater than that of R_{f2} and R_{f4}, peaking at 1.3×10^{-4} hr-ft^2-°F/Btu. The peak fouling resistance occurred approximately 200 cycles sooner for R_{f1} than for R_{f2} and R_{f4}.

The deposit from Run 2 was not photographed. The scale was observed to be of the same type as in Run 1, hard and tenacious. The qualitative judgment was that the scale thickness was less than for Run 1.

The water chemistry for Run 2 was similar to that for Run 1. The average pH was 8.5 and calcium hardness was 144 ppm. The Langelier Index was 1.0.

Experimental Run 3

The thermocouple positions for Run 3 were identical to those of Run 2. The induction time for all three thermocouple locations appears to be approximately 700 cycles. Again, the initial net fouling resistances increased linearly until 1500 cycles, after which

they decreased. The fouling resistances became somewhat constant after 1700 cycles. The values of R_f for all three locations were almost equal throughout the run. The peak magnitude of R_f was 0.55×10^{-4} hr-ft^2-°F/Btu, and the average value during the last 1000 cycles was 0.3×10^{-4} hr-ft^2-°F/Btu.

The scale deposit for Run 3 was photographed macroscopically, and the photographs are shown in Figure 11. It was visually observed that the deposit thickness for Run 3 was less than that of either of the two previous runs, and it was less tenacious.

The water chemistry for Run 3 was also different. The average pH was 7.5 and the average calcium hardness was 170 ppm $CaCO_3$. The Langelier Index was -0.6.

Experimental Run 4

In Run 4 the heat flux was increased to 1616 Btu/hr-ft^2. The average heat flux for the previous three runs was 557 Btu/hr-ft^2. There was no fouling measured at thermocouple locations T_1 and T_4. There was minimal fouling at location T_2, and there appeared to be no peak fouling resistance. The average value of R_{f2} was 0.2 hr-ft^2-°F/Btu.

Scale was visually observed on the heat transfer surface at the extreme edges of the heater, and a very small amount of scale was observed at the thermocouples.

It appears that the water chemistry was the dominant factor in Run 4. The average pH was 7.5 and the average calcium hardness was 177 ppm $CaCO_3$, but the Langelier Index was -1.2.
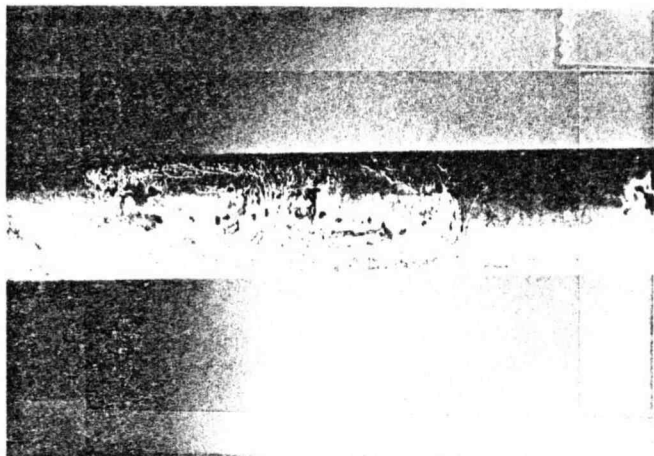
T1 at center

T4 at center
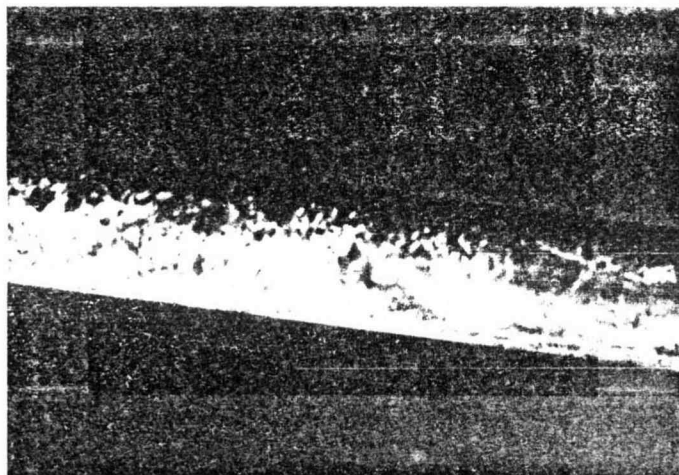
underside view
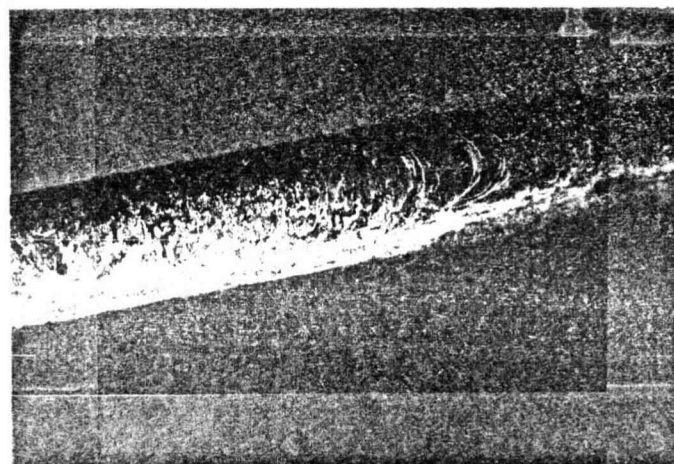
underside view of swirl pattern

Figure 11. Photographs of Deposit on Heat Transfer Surface, Run 3.

The value of R_{f4} decreased for the first 700 cycles, so the value of $1/U_o$ was calibrated to give a zero value of R_{f4} at 700 cycles. A possible explanation for the decrease in R_{f4} is that the heat transfer surface was not entirely clean at the beginning of the run. Since the Langelier Index was negative, the old scale may have redissolved during the initial 700 cycles.

Discussion

Comparisons of Runs 1, 2, and 3

Runs 1, 2, and 3 were designed to compare the effect of the duration of deluge on the fouling behavior. The shapes of the fouling rate curves were similar for the three runs. Following the initial delay time, the net fouling rates were constant for several hundred cycles. Then the resistances declined, and for Run 3, which lasted for more than 3000 cycles, the fouling rates appear to have levelled off at approximately 50% of the peak values. The induction time for Run 1 was slightly longer than for Runs 2 and 3 which were the same. This is probably due to the fact that the surface was new for Run 1 and had been cleaned and roughened before subsequent runs. The duration of the deluge cycle did not appear to significantly affect the induction time.

Although the shapes of the fouling curves were similar, the slopes of the initial fouling rates were not the same from run to run, nor were they the same for different thermocouples within one run. These results support the theory that the rate and magnitude

of the scaling deposit during evaporative fouling on a horizontal cylinder are a function of radial position. Additionally, the rate and magnitude depend on the locations of the initial nucleation sites, since the scale propagates outward from them. The nucleation sites seem to be somewhat dependent on the patterns of the drainage pools. The values of R_f for T_2 and T_4 were often very similar, probably because of their symmetrical locations.

There was a decline in the overall amount of scaling from Run 2 to Run 3. The notable variables between the runs were the pH and methyl alkalinity of the water. Hasson (7) states that a change of one pH unit from pH = 8.8 to pH = 7.7 can increase the solubility of carbonate by as much as one order of magnitude. That would not affect the total scale deposited from evaporation, but it could have an influence on the sensible heat fouling tendency. The values of the Langelier Indices, LSI, for the runs indicate that during the deluge cycles, scaling could have been possible for Run 1, but was questionable for Run 3. Based on the LSI, the magnitude of the scaling should have been greatest for Run 1, as was observed. Since initial nucleation would have occurred in any case due to evaporation fouling, the tendency toward fouling during the deluge cycle was not completely dependent on the LSI but was a function of the local concentration gradient at the nucleation site as well.

The effect of the duration of deluge on the magnitude of the scale deposit could not be determined. Although Run 2 had the longest deluge cycle, Run 1 showed the most scaling. This part of the experiment should have been run at constant water quality

conditions.

Since the magnitude of the scale deposit for this system is a function of the drainage characteristics of the deluge water, the wetting characteristics of the heat transfer surface are probably significant. The wetting capability would affect the holdup time, the film continuity, and the fluid film thickness. Any change in the wettability due to physical treatment of the surface such as cleaning, or in the wetting characteristics of the fluid, would change the initial fluid film layer.

The objective of Run 4 was to determine the effect of increasing the heat flux. There was minimal fouling during Run 4. The increase in heat flux was not expected to influence the total scale deposited during evaporation. In addition, the negative value of the Langelier Index indicates that there may have been a tendency for the deposited calcium carbonate to redissolve during the deluge cycle.

Comparison with Literature

Wheeler et al. (21) studied deposition resulting from deluged wet/dry cooling of aluminum heat exchanger surfaces. A laboratory Corrosion/Deposition Loop (CDL) was used to simulate a cooling tower. It was found that the deposition on the heat exchanger was linearly dependent on concentration factor and number of deluge cycles. It was also found that the rate of fouling was decreased when the heat transfer surface was rinsed with deionized water after deluge, and the decline was attributed to elimination of the evaporative scaling factor.

A comparison of two of Wheeler's runs with Runs 2 and 3 of this study is shown in Table 3. Based on data given in the report (21), a weight gain of 1.0 gm (5.8 mg/dm^2) is approximately equivalent to a scale thickness of 1.25 x 10^{-5} inch. The values of fouling resistances are estimated from Pratt's correlation of R_f vs. scale thickness (14). The Wheeler runs were of one long deluge period, with one drying period at the end of the run. Based on the Table 3 comparison, it appears that for the run at higher pH, the total deluge time, which is the sensible heat contribution, is the pre-dominant factor in scaling. However, at the lower pH the scaling is a function of both the number of deluge cycles, which is the contri-bution due to evaporation, and the total time of deluge.

Wheeler's runs did not extend past 1000 deluge cycles so no com-parison could be made with the observed falling rate portions of the fouling curves for Runs 1, 2, and 3 of the present work.

TABLE 3
COMPARISON OF RUNS 2 AND 3 WITH LITERATURE

Experimental Run	Total Deluge Time (hr)	Number of Deluge Cycles	pH	ppm Ca (as $CaCO_3$)	Wt. gain (gm)	R_f hr-ft^2-°F/Btu
Run 2	250	2000	8.5	144	--	1.3×10^{-4}
Wheeler (20) Run 10	128	1	8.4	69	12.5	(0.5×10^{-4})
Run 3	8	1500	7.5	170	--	0.6×10^{-4}
Wheeler Run 15	120	1	7.5	69	8.1	(0.4×10^{-4})

Note: Values of R_f for the Wheeler Runs are estimated values.

VII. CONCLUSIONS

For the experimental system and operating conditions considered
in this study, it is concluded that:

I. Calcium carbonate scaling of a deluged dry cooling tower
results from a combination of both sensible heat transfer
and evaporation heat transfer mechanisms. The total
amount of scale deposited during evaporation fouling de-
pends on the number of deluge cycles and the deluge water
composition. The total amount of scale deposited during
sensible heat fouling depends on the duration of the
deluge cycles, the temperatures of the deluge water and
the heat transfer surface, and the water quality. It is
possible that under certain conditions of water quality
and temperature, scale that is deposited during the
drying (evaporation) period after deluge may be re-
dissolved during the subsequent deluge cycle.

II. The initial rate of deposition of scale was constant,
but the deposition rate decreased after a certain num-
ber of deluge cycles. Possible causes for the decline
are changes in the wettability of the heat transfer sur-
face or a decrease in the net sensible heat fouling rate.

III. The values of the peak fouling resistances for the same
number of deluge cycles ranged from $R_f = 0.2 \times 10^{-4}$ hr-

ft^2-°F/Btu for Run 4 with Langelier Saturation Index (LSI) of -1.2 to $R_f = 1.3 \times 10^{-4}$ hr-ft^2-°F/Btu for Run 2 with LSI of 1.0.

VIII. SUGGESTIONS FOR FURTHER WORK

The effect of deluge time on scaling should be evaluated at constant water composition. It is possible that an industrial cooling tower could operate with deluge durations of several hours.

Further experimentation is needed in order to determine the shape of the fouling rate curve. It appeared from this study that the fouling behavior followed a falling rate model after 1500 cycles, but it was not determined whether the fouling resistance attained an asymptotic value.

BIBLIOGRAPHY

1. Coates, K. E., "Calcium Carbonate Scaling Characteristics of Cooling Tower Water," M.S. Thesis, Oregon State University, 1980.

2. Epstein, N., "Fouling in Heat Exchangers," Fouling of Heat Transfer Equipment: Proceedings of An International Conference, Hemisphere Publishing, New York, 1981.

3. Epstein, N., "Fouling of Heat Exchangers," Dubrovnik, 1981.

4. Epstein, N., "Fouling: Technical Aspects (Afterword to Fouling in Heat Exchangers)," Fouling of Heat Transfer Equipment: Proceedings of An International Conference, Hemisphere Publishing, New York, 1981.

5. Epstein, N., "Optimum Evaporator Cycles with Scale Formation," Canadian Journal of Chem. Engr., 57:1979, pp. 659-662.

6. Gardner, G. C., "Drainage and Evaporation of a Liquid Film with Salt Deposition upon a Horizontal Cylindrical Surface," International J. Heat and Mass Transfer, Vol. 15, pp. 2063-2075, 1972.

7. Hasson, D., "Precipitation Fouling," Fouling of Heat Transfer Equipment: Proceedings of An International Conference, Hemisphere Publ., New York, 1981.

8. Holman, J. P., Experimental Methods for Engineers, McGraw-Hill, 1978.

9. Kern, D. Q., Seaton, R. E., "Heat Exchanger Design for Fouling Surface," Chem. Engr. Progress, 62(7), pp. 51-56, 1966.

10. Knudsen, J. G., "Fouling of Heat Transfer Surfaces: An Overview," Power Condensor Heat Transfer Technology, Hemisphere Publ., 1981.

11. Knudsen, J. G., "Measurement of Fouling of Heat Transfer Surfaces," Fouling of Heat Transfer Equipment: Proceedings of An International Conference, Hemisphere Publ., New York, 1981.

12. Kunz, R. G., Yen, A. F., Hess, T. C., "Cooling Water Calculations," Chemical Engineering, Aug. 1, 1977.

13. McAdams, W., Heat Transmission, McGraw-Hill, 1954.

14. Pratt, D. R., "Scale Formation in Deluged Dry Cooling Systems," Battelle Pacific Northwest Laboratories, BNWL-2060, UC-12, 1976.

15. Rankin, B. H., Adamson, W. L., "Scale Formation As Related to Evaporator Surface Conditions," Desalination, 13 (1973) pp. 63-87.

16. Roy, B., Experimental work in progress for M.S. Thesis, Oregon State University.

17. Savery, C. W., Bhatti, M. S., "Theory of Augmented Heat Transfer over Finned Surfaces by Fogging," Workshop on Dry Cooling Systems, The Franklin Institute Research Laboratories, 1975.

18. Somerscales, E. F., "Introduction and Summary: The Fouling of Heat Transfer Equipment," Fouling of Heat Transfer Equipment: Proceedings of An International Conference, Hemisphere Publ., New York, 1981

19. Taborek, J., et al., "Fouling: The Major Unresolved Problem in Heat Transfer," Chem. Engr. Progress, 68, pp. 59-67, Feb. 1972, and 68, pp. 69-78, July 1972.

20. Troup, D. H., Richardson, J. A., "Scale Nucleation on a Heat Transfer Surface and Its Prevention," Chem. Engr. Communications, Vol. 2, pp. 167-180, 1978.

21. Wheeler, K. R., et. al., "Deposition and Corrosion Phenomena on Aluminum Surfaces Under Deluged Dry Cooling-Tower Conditions," Battelle Pacific Northwest Laboratories, EPRI CS-1926 Project 422-3 Interim Report, 1981.

APPENDICES

APPENDIX A

NOMENCLATURE

Symbol	Definition
b	A constant
C	Concentration, $lb\text{-}mole/ft^3$
C_{sat}	Saturation concentration at the temperature of the surface, $lb\text{-}mole/ft^3$
C_0, C_1, C_2, C_3	Constants
E	Activation energy, $Btu/lb\text{-}mole$
h, h_0, h_f	Bulk fluid heat transfer coefficients, $Btu/hr\text{-}ft^2\text{-}°F$
k_f	Thermal conductivity of the fouling deposit, $Btu/hr\text{-}ft\text{-}°F$
k_m	Mass transfer coefficient, ft/hr
k_r	First-order attachment/reaction rate constant
$\dot{m}_d$	Rate of formation of the deposit per unit area of fouled surface, $lb_m/hr\text{-}ft^2$
$\dot{m}_r$	Rate of removal of the deposit, $lb_m/hr\text{-}ft^2$
q/A	Heat flux per unit area, $Btu/hr\text{-}ft^2$
R_f	Thermal fouling resistance, $hr\text{-}ft^2\text{-}°F/Btu$
R_g	Gas constant
T	Temperature
U, U_0, U_f	Overall heat transfer coefficient, $Btu/hr\text{-}ft^2\text{-}°F$
x_f	Scale deposit thickness
x/k	Thermal resistance of tube wall, $hr\text{-}ft^2\text{-}°F/Btu$

Appendix A, continued

Symbol	Definition
θ	Time
ϕ_d	Fouling deposition rate, ft^2-°F/Btu
ϕ_r	Fouling removal rate, ft^2-°F/Btu
τ	Wall fluid shear stress, lb_f/ft^2
Ψ	Deposit strength factor
ρ_f	Density of fouling deposit, lb_m/ft^3
Ω	Concentration gradient, lb-mole/ft^3

Subscript	Definition
avg	Average value
b	Bulk conditions
f	Fouled conditions
o	Initial conditions
s	Fouling deposit surface conditions
w	Tube wall conditions

APPENDIX B

CALIBRATION EQUATIONS

The following equations were used in calculating the run data for Appendix E from measured parameters.

Calculation of Heat Flux:

Digital Volt Meter for Power Input (Experimental Equipment)

E = power input to heated rod, in volts

R = resistance of heated rod, in ohms

R = 22.0 ohms

$A = \pi \cdot d \cdot L$ = surface area, in ft^2

d = 0.5/12 ft

L = 0.5 ft

$$q/A = \frac{(E^2/R)}{A} , \quad \text{in watts/ft}^2$$

$$q/A = \frac{(E^2/R)}{A} \cdot (3.413) , \quad \text{in Btu/hr-ft}^2$$

$$q/A = 2.5856 \; E^2$$

Calculation of Temperature:

Digital Millivolt Meter for Temperature Measurement, Chromel-constantin thermocouple (type E)

$$T, \; °F = 32.583 \; (TC + 0.981)^{0.949} \quad \text{for } TC > 3.04$$

$$T, \; °F = 38.529 \; (TC + 0.681)^{0.8765} \quad \text{for } TC < 3.04$$

TC = thermocouple output, in millivolts

Appendix B, continued

Calculation of Water Flow Rate in the Calibration Test Unit:

$$W = 0.4554 \text{ (inches } H_2O)^{0.5370} \quad \text{for Venturi \#270}$$

w = water flow rate, in Gpm

APPENDIX C^{α}

DELUGE WATER QUALITY

TH	CaH	MgH	MA	Cl	pH	Si	TS

January 1982:

| 225. | 150. | 75. | 305. | 464. | 8.7 | 146. | 1160. |

February 1982 (data for 2/22/82 and 2/28/82 only):

| 265. | 180. | 85. | 200. | 400. | 8.6 | 148. | N/A |

March 1982:

| 216. | 144. | 72. | 212. | 376. | 8.5 | 157. | 919. |

April 1982 (after 4/9/82):

| 242. | 168. | 74. | 40. | 482. | 7.5 | 133. | 1067. |

May 1982:

| 247. | 177. | 70. | 10. | 402. | 7.5 | 100. | 754. |

TH $\equiv$ Total hardness, in ppm $CaCO_3$
CaH $\equiv$ Calcium hardness, in ppm $CaCO_3$
MgH $\equiv$ Magnesium hardness, in ppm $CaCO_3$
MA $\equiv$ Methyl alkalinity, in ppm $CaCO_3$
Cl $\equiv$ Chloride (Cl), in ppm
Si $\equiv$ Si(SiO_2), in ppm
TS $\equiv$ Total solids, in mg/litre

$^{\alpha}$Data provided by Roy (16).

Appendix C, continued

CALCULATION OF LANGELIER INDEX

The Langelier Index is a widely used means of predicting the scale forming tendency of calcium carbonate (12). It is derived from the equilibrium relationships of calcium and carbonate in water.

$$HCO_3^- \rightleftharpoons CO_3^{-2} + H^+ \qquad K_2$$

$$Ca^{+2} + CO_3^{-2} \rightleftharpoons CaCO_3(S) \qquad K_{sp}$$
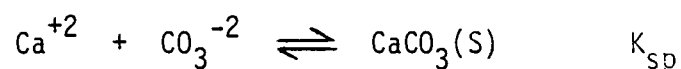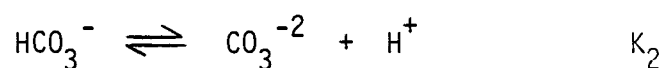
K_2 and K_{sp} are the equilibrium constants and are a function of temperature.

$$[CO_3^{-2}] = \frac{[HCO_3^-]}{[H^+]K_2}$$

$$[Ca^{+2}][CO_3^{-2}] = K_{sp}$$

therefore at saturation conditions

$$[H^+]_s = \frac{[Ca^{+2}][HCO_3^-]}{K_2 K_{sp}}$$

The Langelier Index compares the solution pH with the saturation pH

$$LSI = pH - pH_s = pH - (pCa + pHCO_3^- - pK_2 - pK_{sp})$$

If the value of LSI is positive, the water is supersaturated and scale can deposit, whereas if the value is negative the tendency is for calcium carbonate to dissolve (12).

Appendix C, continued

For Runs 1, 2, 3, and 4, the values for pH, pCa^{+2}, and $pHCO_3^-$ can be obtained from the water quality data for pH, calcium hardness, and methyl alkalinity, respectively. The values of the equilibrium constants at 90°F are (12):

$$K_2 = 4.7 \times 10^{-11}$$

$$K_{sp} = 4.5 \times 10^{-9}$$

The values of the Langelier Indices for the water of Runs 1, 2, 3, and 4 are:

Run 1	(Jan./Feb.)	LSI = 1.4
Run 2	(March)	LSI = 1.0
Run 3	(April)	LSI = -0.6
Run 4	(May)	LSI = -1.2

APPENDIX D

RUN RESULTS

Run 1, Conditions

Run Conditions (Experimental Unit)

Cycle: Duration of Deluge = 2.0 min.

Drying Interval = 10.0 min.

Heat Flux: power E_{avg} = 14.6 volts $\pm$ 0.5 volts

$(q/A)_{avg}$ = 550.24 Btu/hr-ft^2

Appendix D.   Run 1, Clean Conditions

q/A Btu/hr-ft^2	T_b °F	T_2	T_3 °F	T_4
549.6	60.26	89.6	89.4	89.9
542.1	59.41	88.9	88.8	89.2
543.6	59.15	89.4	89.3	89.6
565.5	55.32	88.9	88.8	89.2

$1/U_{avg}$, hr-ft^2-°F/Btu

$1/U_2 = 0.055799$

$1/U_3 = 0.055600$

$1/U_4 = 0.056304$

$1/U_{avg}$, hr-ft^2-°F/Btu

$1/h_2 = 0.055603$

$1/h_3 = 0.055571$

$1/h_4 = 0.056238$

Note: The measurements were taken on the Experimental Equipment. The bulk fluid was humid air, and the temperature measured was the wet bulb temperature at the inlet. The clean conditions were measured at the end of Run 1, 3/2/82 and 3/3/82, after the cylinder had been cleaned.

Appendix D. Run 1, Summary of Data

Date	Number of Cycles	q/A (Btu/hr-ft^2)	T_b [a] (°F)	T_2	T_3 (°F)	T_4 [b]	$R_{f2} \times 10^4$	$R_{f3} \times 10^4$ (hr-ft^2-°F/Btu)	$R_{f4} \times 10^4$
1/29/82	887	528.7	60.26	88.8	89.7	90.6	-11.6	7.8	17.7
1/31/82	1127	528.7	58.38	87.4		90.3	-14.3		36.2
2/1/82	1237	525.0	54.07	87.4	85.8	88.6	59.6	31.2	78.4
2/1/82	1282	536.1	55.03	87.1	85.6	90.1	26.7	2.2	78.6
2/3/82	1522	525.0	53.54	87.0	85.8	86.4	61.3	39.8	43.4
2/4/82	1582	536.1	53.38	85.4	85.8	86.3	20.5	29.4	30.5
2/6/82	1707	536.1	52.69	86.0	84.0	84.8	29.2	8.6	13.2
2/8/82	1920	536.1	49.54	82.1	81.1	81.9	15.0	- 2.2	6.1
2/8/82	1955	543.6	51.98	83.4	82.0	83.0	- 5.2	-28.3	-17.8
2/9/82	2025	539.8	51.92	83.6	82.1	83.8	4.1	-21.3	2.1
2/9/82	2050	519.5	52.26	83.7	83.0	84.0	23.0	12.2	23.5
2/10/82	2120	501.3	51.25	83.8	83.6	84.3	62.8	61.8	67.7
2/11/82	2235	538.3	55.38	85.2	84.7	85.4	-15.6	-22.0	-16.6
2/11/82	2270	530.9	55.63	87.7	87.1	87.8	35.2	25.5	33.1
2/12/82	2352	523.5	56.28	87.3	87.2	87.8	27.5	26.3	31.0
2/14/82	2585	539.8	62.82	89.8	89.8	90.1	-42.2	-39.7	-40.4
2/14/82	2610	532.4	62.60	89.7	89.5	89.9	-33.8	-35.8	-33.9
2/16/82	2850	538.3	61.21	89.4	89.3	89.8	-23.9	-24.1	-21.0
2/17/82	2905	512.5	58.90	88.7	88.6	89.2	25.1	25.9	29.5
2/17/82	2915	537.6	59.09	88.2	89.8	90.2	-12.8	17.5	18.7
2/17/82	2925	537.6	58.99	89.1	89.2	89.8	3.8	8.6	11.6

[a] For 1/29/82 - 2/8/82, T_b based on measurements of T_d-inside, corrected to T_{wb}-inlet.
For 2/9/82 - 2/17/82, T_b = T_{wb}-inlet.

[b] All temperatures were measured with the deluge water on.

Appendix D. Run 1, Observations

<u>Date</u>

2/6/82

Comments

T_4

T_2
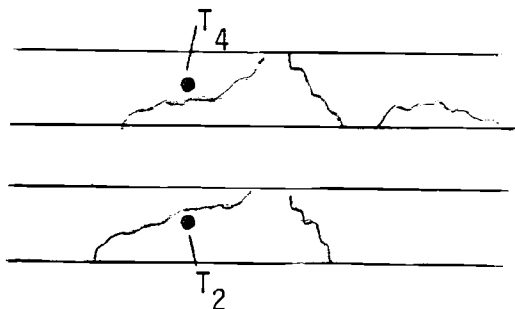
overall

1. Scale was visually observed at the thermo-couple locations 2 and 4 at approximately 1000 cycles. No scale was observed at T3 at this time, although the data indicates a positive value for R_{f3}.

2. Scale was initially visually observed at approximately 500 cycles at the bottom of both ends of the heated section. The scale then propagated inward and around the cylinder from these two locations. Scale also propagated from the bottom at other locations between the two ends.

3. At the end of the run, the scale had not completely covered the heated surface.

4. The scale was very tenacious and required removal by a metal file. The deposit could not be removed with water, and there was minimal flaking.

Appendix D. Run 2, Conditions

Run Conditions (Experimental Unit)

Cycle: Duration of Deluge = 8.0 min.
    Drying Interval   = 10.0 min.

Heat Flux: power E_{avg} = 14.45 volts $\pm$ 0.5 volts

$(q/A)_{avg}$ = 539.8 Btu/hr-ft^2

Test Conditions (Calibration Test Unit)

q = 500 watts

q/A = 28441. Btu/hr-ft^2

inches H_2O = 70.0 , Venturi #270

W = 4.474 gpm, flow rate of water

Appendix D. Run 2, Clean Conditions

Experimental Unit Clean Conditions
(measured on 3/4/82, beginning of Run 2)

q/A = 551.1 Btu/hr-ft^2

T_b = 0.86   mV = 56.28 °F

T1	T2	T4
	millivolts	
1.908	1.921	1.913
1.907	1.920	1.912
1.906	1.919	1.911
1.903	1.916	1.910
1.906	1.917	1.909
1.904	1.918	1.910
1.903	1.917	1.908
1.904	1.917	1.907
1.899	1.913	1.905
1.897	1.912	1.904
1.899	1.912	1.904
1.899	1.912	1.904
1.903	1.916	1.908

$T1_{avg}$ = 88.54 °F

$T2_{avg}$ = 88.93 °F

$T4_{avg}$ = 88.69 °F

$1/U_{avg}$, hr-ft^2-°F/Btu

$1/U_1$ = 0.058526

$1/U_2$ = 0.059248

$1/U_4$ = 0.058804

$1/U_{avg}$, hr-ft^2-°F/Btu

$1/h_1$ = 0.058497

$1/h_2$ = 0.059182

$1/h_4$ = 0.058607

Calibration Test Unit Clean Conditions
(measured on 4/8/82, at the end of Run 2, after the cylinder had
  been cleaned)

The data and calculations are the same as those for Run 3 clean
conditions.

Appendix D. Run 2, Summary of Data

Date	Number of Cycles	q/A (Btu/hr-ft^2)	T_b ($°F$)	T_1	T_2 ($°F$)	T_4	$R_{f1} \times 10^4$	$R_{f2} \times 10^4$ (hr-ft^2-$°F$/Btu)	$R_{f4} \times 10^4$
3/8/82	280	543.6	8.52	89.2	89.4	89.1	-20.61	-23.69	-23.94
3/13/82	680	557.2	59.50	91.4	91.7	91.3	- 8.19	-10.53	-12.57
3/15/82	840	537.6	57.78	95.2	95.4	95.0	107.79	105.51	101.69
3/17/82	1000	522.0	54.03	91.0	91.3	90.8	105.16	104.02	98.90

-------- Changed measuring technique from Experimental Unit to Calibration Unit --------------------

Date	Number of Cycles	q/A (Btu/hr-ft^2)	T_b ($°F$)	T_1	T_2 ($°F$)	T_4	$R_{f1} \times 10^4$	$R_{f2} \times 10^4$ (hr-ft^2-$°F$/Btu)	$R_{f4} \times 10^4$
3/19/82	1160		50.13	97.2	93.3	98.4	1.10	0.27	0.42
3/28/82	1870		70.76	109.7	114.1	112.9	1.36	0.57	0.49
3/31/82	2025		69.46	107.7	113.2	111.7	1.00	0.61	0.44
4/1/82	2100		68.43	107.1	112.0	111.7	1.08	0.47	0.72
4/5/82	2420		66.06	105.0	110.6	109.7	1.01	0.58	0.65
4/6/82	2500		67.37	105.6	110.9	110.0	0.86	0.34	0.40

Appendix D.   Run 2, Observations

<u>Date</u>   <u>Comments</u>

3/19/82
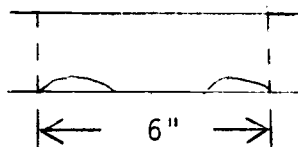
induction periods for Run 1 and Run 2
are not significantly different.

overall   1.   Scaling profile on the heat transfer surface
                          is similar to Run 1. There is scale on both
                          ends, either side of heater, and on the bottom
                          center.

                     2.   Nucleation began on the bottom and spread up-
                          wards. The scale is formed in "rings" and
                          "swirls."

                     3.   The scale thickness appears to be less than
                          for Run 1.

                     4.   Thermocouple locations:
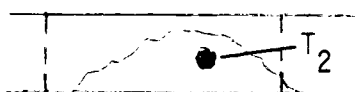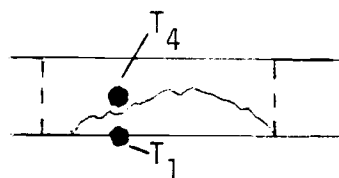
Appendix D. Run 3, Conditions

Run Conditions (Experimental Unit)

    Cycle: Duration of Deluge = 1/3 min.
             Drying Interval   = 10.0 min.

    Heat Flux: power E_{avg} = 15.0 volts $\pm$ 0.5 volts
            $(q/A)_{avg}$ = 581.7 Btu/hr-ft^2

Test Conditions (Calibration Test Unit)

    q = 500 watts

  q/A = 28441. Btu/hr-ft^2

  inches H_2O = 70.0 , Venturi #270

  W = 4.474 Gpm, flow rate of water

Appendix D. Run 3, Clean Conditions

q/A Btu/hr-ft^2	T_b °F	T_1 °F	ΔT_1 °F	T_2 °F	ΔT_2 °F	T_4 °F	ΔT_4 °F
28441.	68.09	103.5	35.50	110.32	42.23	109.45	41.35
28441.	68.34	103.8	35.55	110.90	42.56	109.45	41.10
28441.	68.46	104.1	35.71	110.90	42.44	109.74	41.27
28441.	68.65	104.1	35.53	110.90	42.25	109.74	41.08
28441.	68.77	104.1	35.40	110.90	42.12	110.03	41.25
28441.	68.90	104.1	35.28	110.90	42.00	110.03	41.13
28441.	68.93	104.4	35.54	111.19	42.26	110.32	41.39
28441.	69.15	104.7	35.62	111.19	42.04	110.32	41.17
28441.	69.27	104.7	35.49	111.19	41.92	110.32	41.04
28441.	69.40	105.0	<u>35.66</u>	111.49	<u>42.08</u>	110.61	<u>41.21</u>
			35.53		42.19		41.20

$1/U_{avg}$, hr-ft^2-°F/Btu

$1/U_1 = 0.0012493$

$1/U_2 = 0.0014836$

$1/U_4 = 0.0014488$

$1/h_{avg}$, hr-ft^2-°F/Btu

$1/h_1 = 0.0012205$

$1/h_2 = 0.0014179$

$1/h_4 = 0.0012524$

Note: The measurements were taken on the Calibration Test Unit on 4/8/82, at the beginning of Run 3.

Appendix D.   Run 3, Summary of Data

Date	Number of Cycles	T_b °F	T_1 °F	T_2 °F	T_4 °F	$R_{f1} \times 10^4$	$R_{f2} \times 10^4$	$R_{f4} \times 10^4$
						--------	hr-ft^2-°F/Btu	-------
4/9/82	140	70.58	105.6	112.3	111.6	0	0	0
4/10/82	280	73.00	107.4	114.1	113.2	0	0	0
4/12/82	490	70.06	104.7	111.4	110.6	-0.20	-0.20	-0.20
4/13/82	630	68.80	103.8	110.4	110.3	-0.07	-0.10	+0.14
4/14/82	700	66.60	104.1	109.8	110.4	0.18	0.18	0.76
4/15/82	840	67.54	103.8	110.0	109.4	0.19	0	0.14
4/15/82	906	69.68	104.7	111.9	110.9	-0.08	0.09	0.07
4/18/82	1255	67.23	104.1	111.0	109.7	0.38	0.43	0.33
4/18/82	1325	69.09	105.9	112.6	111.4	0.49	0.50	0.44
4/19/82	1394	65.75	103.0	110.3	109.1	0.37	0.56	0.53
4/19/82	1464	68.28	104.6	112.0	110.4	0.25	0.51	0.30
4/20/82	1533	68.81	105.6	112.3	111.4	0.54	0.54	0.55
4/21/82	1743	75.05	110.0	116.7	115.5	0.27	0.34	0.22
4/22/82	1812	76.16	110.3	117.5	116.4	0.06	0.34	0.22
4/23/82	1952	74.08	109.3	115.6	114.8	0.28	0.24	0.24
4/24/82	2021	72.65	107.9	114.6	113.5	0.22	0.27	0.17
4/25/82	2126	72.16	107.9	114.6	113.5	0.36	0.40	0.31
4/26/82	2265	68.68	104.7	111.7	110.9	0.19	0.30	0.35
4/27/82	2400	70.45	106.5	112.6	112.0	0.32	0.14	0.27
4/29/82	2720	65.37	102.4	109.4	108.2	0.27	0.35	0.32
5/2/82	3100	54.10	94.7	101.5	100.5	0.56	0.40	0.56

Appendix D. Run 3, Observations

Date   Comments

4/9/82   1. There is already visible scale on the bottom
                    center and edges of the heated surface.

                2. The brass cylinder is becoming increasingly
                    rougher as it is cleaned between runs.

4/10/82   Scale observed at location T1.

5/1/82   Scale observed at all thermocouple locations.

overall   There was less scale than on previous runs.
                The scale was less tenacious, was more flakey,
                and some of it could be rubbed off.

Appendix D. Run 4, Conditions

Run Conditions (Experimental Unit)

Cycle: Duration of Deluge = 1.0 min.
        Drying Interval   = 10.0 min.

Heat Flux: power E_{avg} = 25.0 volts $\pm$ 0.5 volts

$(q/A)_{avg}$ = 1616.0 Btu/hr-ft^2

Test Conditions (Calibration Test Unit)

q = 500 watts

q/A = 28441. Btu/hr-ft^2

inches H_2O = 70.0 , Venturi #270

W = 4.474 Gpm, flow rate of water

Appendix D. Run 4, Clean Conditions

q/A Btu/hr-ft^2	T_b °F	T_1 °F	ΔT_1 °F	T_2 °F	ΔT_2 °F	T_4 °F	ΔT_4 °F
28441.	56.99	96.2	39.2	103.3	46.3	101.8	44.8
28441.	56.99	96.2	39.2	103.3	46.3	101.8	44.8

$1/U_{avg}$, hr-ft^2-°F/Btu

$1/U_1 = 0.0013793$

$1/U_2 = 0.0016285$

$1/U_4 = 0.0015768$

$1/h_{avg}$, hr-ft^2-°F/Btu

$1/h_1 = 0.0013504$

$1/h_2 = 0.0015629$

$1/h_4 = 0.0013804$

Note: The measurements were taken on the Calibration Test Unit on 5/11/82.

Appendix D. Run 4, Summary of Data

Date	Number of Cycles	T_b	T_1	T_2	T_4	$R_{f1} \times 10^4$	$R_{f2} \times 10^4$	$R_{f4} \times 10^4$
		--------------- °F ---------------				------- hr-ft^2-°F/Btu --------		
5/7/82	250	63.46	101.5	108.1	110.3	0.17	0.08	1.27
5/8/82	310	63.27	100.5	107.5	110.0	-0.14	-0.08	1.24
5/10/82	572	67.03	103.4	110.4	112.5	-0.12	-0.04	1.10
5/11/82	736	56.99	96.2	103.3	101.8	0	0	0
5/13/82	943	59.76	98.3	105.6	104.2	0	0.14	0.11
5/14/82	1074	64.59	101.8	109.4	107.7	-0.04	0.25	0.06
5/15/82	1200	60.52	98.6	106.2	104.5	-0.09	0.15	0.01
5/16/82	1336	59.66	98.0	105.9	103.9	-0.07	0.26	0.03
5/17/82	1461	62.04	99.5	107.1	105.3	-0.18	0.08	-0.08
5/27/82	2770	59.54	98.0	106.2	103.3	0	0.29	0

APPENDIX E

TEMPERATURE STUDIES

Appendix E.1.

STUDY OF BULK FLUID CONDITIONS INSIDE THE COLUMN

In a deluge dry cooling system, the bulk fluid cooling medium is air of variable humidity. As the air flows past the heat transfer surface, the dry bulb temperature increases. The change in wet bulb temperature is a function of the inlet wet bulb temperature and relative humidity, the velocity, and whether the heated surface is dry or wet. The influence of the humidity factor at constant velocity was studied to determine the best choice of bulk fluid temperature measurement. The data for Run 1 are summarized in Table i and Figure i.

As indicated in the Table, the inlet wet bulb temperature was the most consistent T_b over the time period. The difference between the wet and dry bulb temperatures at the inlet was greatest on those days when the dry bulb temperature was the highest, and that was also true with the difference between the wet bulb and dry bulb temperatures inside the column above the heated surface.

The values of the fouling resistance, R_f, for Run 1 were calculated based on T_b for the inlet wet bulb temperature. However, the probability of that measurement accurately representing the bulk fluid temperature was of error magnitude greater than the magnitude of R_f. An error of ± 2 °F in either the bulk temperature or the change in bulk temperature as the air flows past the heated surface will cause an average change of ± 0.0035 hr-ft^2-°F/Btu in R_f. That error is larger than the magnitude of R_f. The problem is more

important for humid air than for water for two reasons. There can actually be a greater temperature change in the bulk fluid due to the humidity change than the temperature change due to fouling resistance. Also, the heat transfer coefficient for air is much lower than for water, and thus any error in 1/h will have a greater influence on the calculation of R_f.

Because of the uncertainty in T_b, the temperature measurements for Runs 2, 3, and 4 were made in the Calibration Test Unit. The velocity and heat flux were constant for all measurements, and the bulk fluid was water.

Table i. Bulk Fluid Temperature Measurements.

Date	Volts	Wet Bulb Temperature, °F			Dry Bulb Temperature, °F		
		Inlet	Inside, W.on	Inside, W.off	Inlet	Inside, W.on	Inside, W.off
2/8/82	14.20	58.39			66.25		
	14.40	58.99			68.18		
	14.50		61.43			63.26	
2/9/82	14.45		61.37			66.18	
	14.20		61.72			63.17	
2/10/82	13.90		60.71			63.30	
2/11/82	14.43		64.84	62.19		67.34	
	14.33		65.09	62.10		68.12	
2/12/82	14.23	56.28	64.24	56.28		68.21	
2/14/82	14.45	62.82	73.39	66.72	73.39		
	14.35	62.60			73.17		
2/16/82	14.43	61.21			73.36		
2/17/82	14.10	58.90			71.47		
	14.42	59.09			72.93		
	14.42	58.99			74.75		
	14.35	59.31			75.33		
3/2/82	14.58	60.26	69.96	63.52	70.70		
	14.48	59.41	68.96	62.73	69.89		75.02
3/3/82	14.50	59.15	68.56	63.26			
	14.75	55.32	64.43	57.37	64.84	69.96	
3/4/82	14.55	56.28	66.37	58.32	66.78		72.62
3/5/82	14.35	56.76	68.06	58.45	65.75		70.02
3/8/82	14.50	58.52	68.34	61.50	62.68		68.06
3/13/82	14.68	59.50	66.34	62.54	66.03		
3/15/82	14.42	57.78	65.71		65.78	70.23	
3/17/82	14.20	54.03	64.52	57.40	68.43	72.56	
3/19/82	14.45	56.60	66.75		66.87		
mean, $\bar{x}$	14.39	58.58	65.83	60.95	69.29	67.23	71.43
standard deviation, σ	0.176	2.20	3.28	3.08	3.78	3.25	3.03
variance, σ^2	0.031	4.84	10.78	9.53	14.30	10.59	9.22

WATER ON: ΔT

Wet Bulb $(T_{b2}-T_{bl})$:
$\bar{x} = 9.4543$ °F
$\sigma = 1.2350$ °F

Dry Bulb $(T_{b2}-T_{bl})$:
$\bar{x} = 4.5672$ °F
$\sigma = 0.5059$ °F

$T_{b2-inside}$

Wet Bulb: $\bar{x} = 67.0414$ °F
(water on) $\sigma = 2.5351$ °F

Wet Bulb: $\bar{x} = 60.9571$ °F
(water off) $\sigma = 3.0879$ °F

$T_{bl-inlet}$

Wet Bulb: $\bar{x} = 59.0223$ °F
$\sigma = 2.2580$ °F

Dry Bulb: $\bar{x} = 68.3740$ °F
$\sigma = 4.0300$ °F

WATER ON: ΔT

$(T_{b2-inside-dry\ bulb} - T_{b2-inside-wet\ bulb})$
$\bar{x} = 4.5986$ °F
$\sigma = 1.9950$ °F
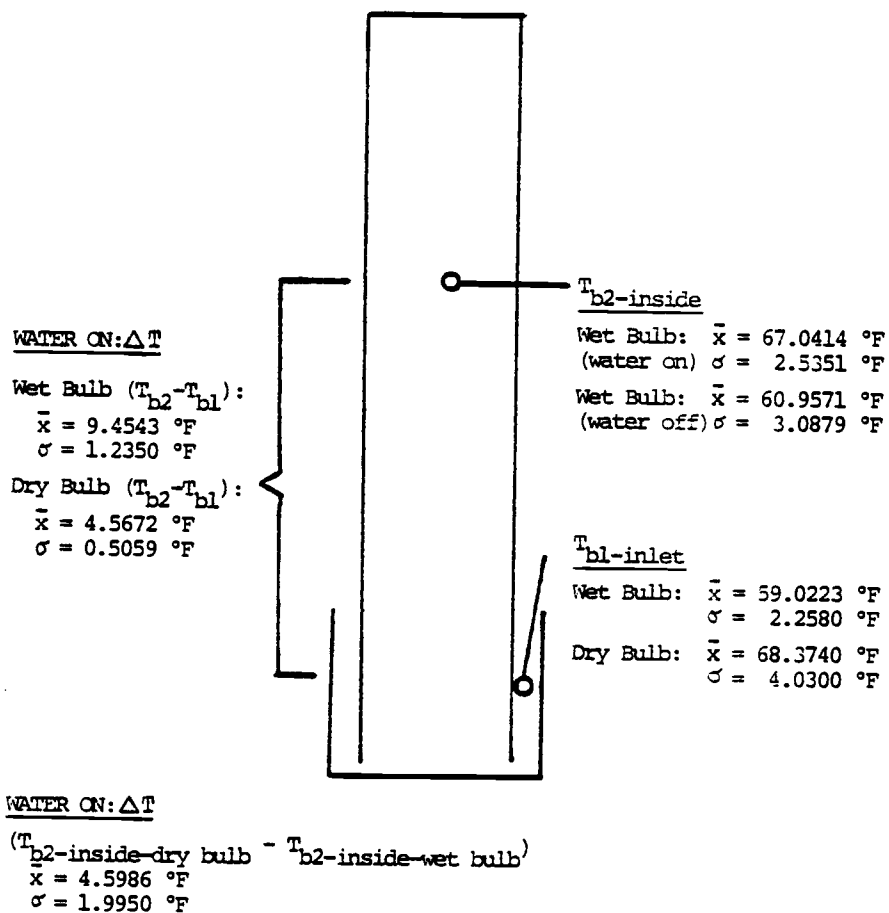
Figure i. Summary of Typical Bulk Fluid Conditions Inside the Column,
$\bar{x}$ = mean temperature, σ = standard deviation.

Appendix E.2.

BULK TEMPERATURE STUDY

The calculation of fouling resistance is a function of the mea-
sured bulk fluid temperature according to Equation (29):

$$R_f = \frac{1}{U_f} - \frac{1}{U_o} - \frac{1}{h_o} [(\frac{1+0.011T_{bo}}{1+0.011T_b}) - 1]$$

where T_{bo} is the initial temperature measured at the clean conditions
and T_b is the temperature measured at the fouled conditions. In order
to test the validity of this assumption, measurements of T_w as a
function of T_b were taken at the end of Run 3. These values were
used to calculate R_f according to the above equation. Assuming R_f
to be constant over a small temperature range, the predicted values
should be the same at all values of T_b. The results are shown in
Table ii.

The values for the mean fouling resistance, $\bar{R}_f$, are very close
to the values calculated at T_{bo}, and the standard deviation, σ, is
much less than the predicted maximum error for R_f of 0.000014 hr-ft^2-
°F/Btu. Also, since there is little correlation between T_b and pre-
dicted R_f, then it is concluded that R_f is not a function of T_b over
this temperature range.

Table ii. Bulk Temperature Study[a]

T_b	T_1	T_2	T_4	$R_{f1}\times10^4$	$R_{f2}\times10^4$	$R_{f4}\times10^4$
68.37	104.4	111.4	110.3	0.17	0.28	0.23
68.68[b]	104.7	111.7	110.9	0.19	0.30	0.35
69.21	105.6	112.0	111.1	0.15	0.26	0.30
69.52	105.3	112.3	111.4	0.16	0.29	0.32
69.83	105.6	112.3	111.7	0.18	0.20	0.34
69.99	105.9	112.6	112.0	0.24	0.26	0.40
70.14	106.2	112.9	112.0	0.25	0.33	0.36
70.55	106.5	113.2	112.3	0.24	0.32	0.35
70.82	106.5	113.2	112.6	0.22	0.25	0.37
71.07	106.8	113.5	112.6	0.20	0.28	0.30
71.38	107.1	113.8	112.9	0.22	0.40	0.32
71.69	107.1	114.1	112.9	0.18	0.32	0.24
72.00	107.4	114.1	113.2	0.20	0.24	0.25
72.31	107.7	114.3	113.5	0.21	0.26	0.27
72.62	107.9	114.6	113.8	0.23	0.28	0.29
72.93	108.2	114.9	114.1	0.25	0.30	0.30
			mean, $\bar{x}$	0.20	0.28	0.31
			standard deviation, σ	0.032	0.045	0.049
	for $x=T_b$ {	correlation coefficient, r		0.45	0.11	-0.27
	$y=R_f^b$	slope, m		0.000001	0.0000004	-0.000001

[a]Experimental conditions (Calibration Test Unit)
    1. date measured 4/26/82
    2. q/A = 28441. Btu/hr-ft^2
        G = 4.4739 Gpm

[b]Value of T_b closest to T_{bo} = 68.80

Appendix E.3.

COMPARISON OF WALL TEMPERATURES, WATER ON OR OFF

The wall temperature T_1 was measured as a function of time after water was turned on or off in the Experimental Unit. The results are summarized in Figure ii.

For heat fluxes ranging from 540 Btu/hr-ft^2 to 2327 Btu/hr-ft^2, the wall temperature never exceeded 120°F during any part of the deluge cycle, indicating that the deluge water temperature did not ever exceed 120°F. Almost immediately after the water was turned on, the wall temperature dropped to less than 100°F. This was true even in the extreme case where the wall temperature reached 300°F during the drying interval. Sensible heat fouling, if it occurs, occurs during the deluge cycle. Therefore, for the heat fluxes and system considered here, any sensible heat fouling would have to occur at water temperatures of 90-100°F.
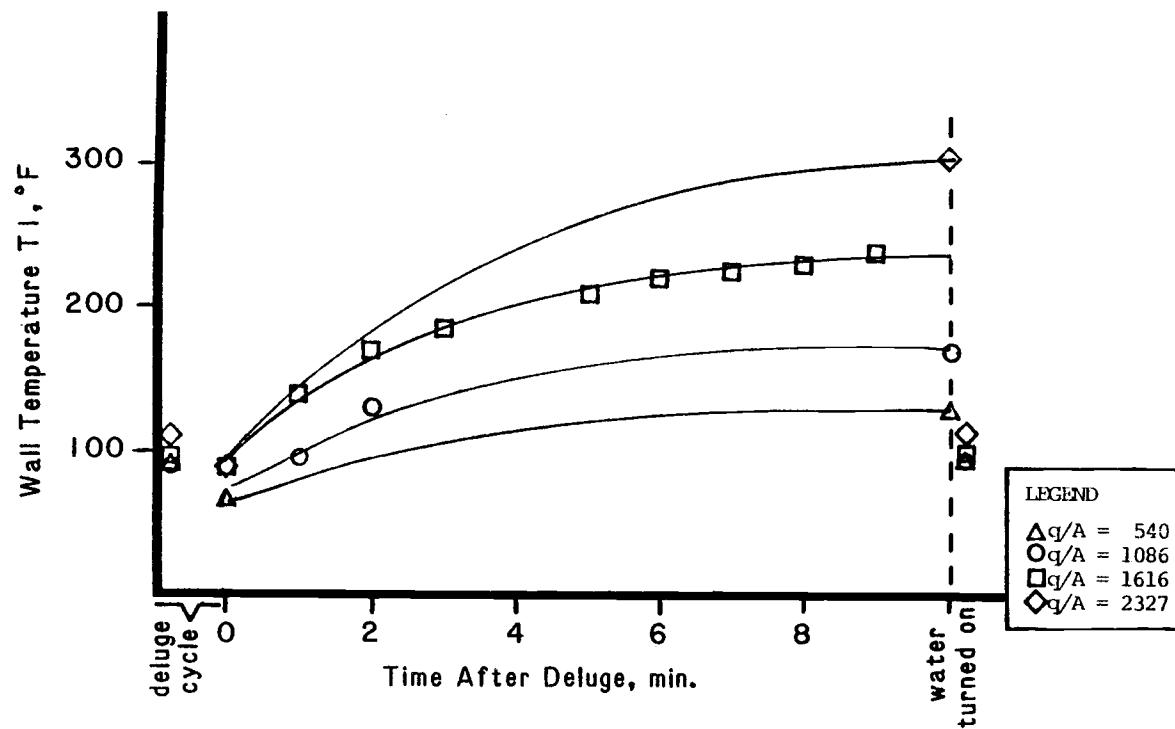
Figure ii. Comparison of Wall Temperatures